Εθνικό & Καποδιστριακό Πανεπιστήμιο Αθηνών
Τμήμα Βιολογίας
Τομέας Βοτανικής
Αθήνα, 2016

Διπλωματική εργασία: Γεωργία Σιούπουλη 1113201100108
Υπεύθυνος Καθηγητής: Γιώργος Διαλλινάς

Μέρος Α: Cryptic purine transporters in *Aspergillus nidulans* reveal the role of specific residues in the evolution of specificity in the NCS1 family

Μέρος Β: Design and synthesis of purine analogues as highly specific ligands for FcyB, a ubiquitous fungal nucleobase transporter

Περιεχόμενα

Περίληψη

Οι μεταφορείς NCS1 είναι υπεύθυνοι για την πρόσληψη πουρινών, πυριμιδινών και αναλόγων τους, με αντιπροσώπους στα βακτήρια, τους μύκητες και αρκετά φυτά. Τα μέλη της NCS1 των μυκήτων έχουν κατηγοριοποιηθεί σε δύο υποοικογένειες, την Fcy και την Fur, με βάση διαφορές στην δομή και την εξειδίκευση της λειτουργίας τους, αλλά και την εξελικτική τους απόκλιση. Η Fur υποοικογένεια του *Aspergillus nidulans* χαρακτηρίστηκε πρόσφατα και περιλαμβάνει γονίδια που κωδικοποιούν για βασικούς μεταφορείς εξειδικευμένων στην πρόσληψη ουρακίλης, 5-φθοροουρακίλης και αλλαντοΐνης, αλλά και για δευτερεύοντες «κρυπτικούς» μεταφορείς με διευρυμένη ικανότητα αναγνώρισης και άλλων νουκλετιδικών βάσεων, όπως το ουρικό οξύ. Από την οικογένεια Fcy του *A. nidulans*, μόνο η πρωτεΐνη FcyB έχει χαρακτηριστεί ως συμμεταφορέας H^+/ πουρινών-κυτοσίνης . Στην παρούσα εργασία αναζητήσαμε την λειτουργία των υπολοίπων Fcy μεταφορέων (Fcy-A, -C, -D, -E) του *A. nidulans*. Χαρακτηρίσαμε πλήρως τον FcyD ως μεταφορέα μέσης-συγγένειας και χαμηλής-μεταφορικής ικανότητας, αλλά υψηλής-εξειδίκευσης για την αδενίνη, ενώ παρουσιάζουμε στοιχεία που δείχνουν ότι ο FcyE συνεισφέρει στην πρόσληψη γουανίνης. Αντίθετα, δεν βρέθηκε ο ρόλος των FcyC και FcyA. Μελετήσαμε παραιτέρω τις σχέσεις δομής-λειτουργίας του FcyD μέσω κατευθυνόμενης μεταλλαξιγένεσης και ταυτοποιήσαμε δύο συντηρημένα αμινοξικά κατάλοιπα (Leu356 και Ser359) στο διαμεμβρανικό τμήμα 8 (TMS8) ως καθοριστικής σημασίας για την εξειδίκευση του FcyD. Επιπλεόν αναγνωρίσαμε δύο σημαντικά για την λειτουργία του FcyD αμινοξικά κατάλοιπα (Phe167 και Ser171) στο διαμεμβρανικό τμήμα 3 (TMS3). Τέλος, αξιοσημείωτο είναι πώς η μεταλλαγή S359N μετέτρεψε τον μεταφορέα FcyD σε ένα διευρυμένης εξειδίκευσης μεταφορέα νουκλεοτιδίων. Τα αποτελέσματα μας αποκαλύπτουν τη σημαντικότητα των ειδικών αμινοξικών κατάλοιπων στην λειτουργική εξέλιξη των NCS1 μεταφορέων.

* Η εργασία αυτή πραγματοποιήθηκε στα πλαίσια συνεργασίας και από το άρθρο αυτό είμαι υπεύθυνη για τις εξής εικόνες: 2A, 2B, 3A, 3B, 3C, 4A, 4B, 5A, 5B, 5C.

Molecular Microbiology (2016) 00(00), 00–00 ■

doi:10.1111/mmi.13559
First published online 00 Month 2016

Cryptic purine transporters in *Aspergillus nidulans* reveal the role of specific residues in the evolution of specificity in the NCS1 family

AQ2

Georgia Sioupouli,[1] George Lambrinidis,[2] Emmanuel Mikros,[2] Sotiris Amillis[1]* and George Diallinas[1]*

[1]*Department of Biology, National and Kapodistrian University of Athens, Panepistimioupolis Athens 15784, Greece.*

[2]*Department of Pharmacy, National and Kapodistrian University of Athens, Panepistimioupolis Athens 15771, Greece.*

Summary

NCS1 proteins are H^+ or Na^+ symporters responsible for the uptake of purines, pyrimidines or related metabolites in bacteria, fungi and some plants. Fungal NCS1 are classified into two evolutionary and structurally distinct subfamilies, known as Fur- and Fcy-like transporters. These subfamilies have expanded and functionally diversified by gene duplications. The Fur subfamily of the model fungus *Aspergillus nidulans* includes both major and cryptic transporters specific for uracil, 5-fluorouracil, allantoin or/and uric acid. Here we functionally analyse all four *A. nidulans* Fcy transporters (FcyA, FcyC, FcyD and FcyE) with previously unknown function. Our analysis shows that FcyD is moderate-affinity, low-capacity, highly specific adenine transporter, whereas FcyE contributes to 8-azaguanine uptake. Mutational analysis of FcyD, supported by homology modelling and substrate docking, shows that two variably conserved residues (Leu356 and Ser359) in transmembrane segment 8 (TMS8) are critical for transport kinetics and specificity differences among Fcy transporters, while two conserved residues (Phe167 and Ser171) in TMS3 are also important for function. Importantly, mutation S359N converts FcyD to a promiscuous nucleobase transporter capable of recognizing adenine, xanthine and several nucleobase analogues. Our results reveal the importance of specific residues in the functional evolution of NCS1 transporters.

AQ3 Accepted ***. *For correspondence. E-mail samillis@biol.uoa.gr; dialling@biol.uoa.gr

© 2016 John Wiley & Sons Ltd

Introduction

Purines, pyrimidines and related analogues and drugs are transported in both prokaryotic and eukaryotic cells through the action of specific plasma membrane transporters (De Koning and Diallinas, 2000; Pantazopoulou and Diallinas, 2007; Frillingos, 2012; Young *et al.*, 2013; Girke *et al.*, 2014). In bacteria, fungi and plants, two families are highly specific for purines and pyrimidines. These are known as the NAT/NCS2 (nucleobase ascorbate transporters or nucleobase cation symporter family 2) and NCS1 (nucleobase cation symporter family 1) families. The NAT family is also present in metazoa, but in primates NAT members have evolved to become L-ascorbate rather than nucleobase transporters (Diallinas and Gournas, 2008; Gournas *et al.*, 2008; Frillingos, 2012; Alguel *et al.*, 2016). Fungal NCS1 transporters have been further classified, based on their primary amino acid sequences and specificity profiles into two structurally and functionally distinct subfamilies, the Fcy-like and the Fur-like transporters (De Koning and Diallinas, 2000; Pantazopoulou and Diallinas, 2007). A recent phylogenetic analysis has shown that Fur and Fcy, and their plant homologues, originate through independent horizontal transfers from prokaryotes, and that gene duplication has led to the multiplication and functional diversification of fungal NCS1 (Krypotou *et al.*, 2015).

Functionally characterised fungal Fur-like proteins are high-affinity H^+ symporters, specific for allantoin, uracil, uridine, thiamine, nicotinamide riboside and secondarily for uric acid and xanthine (Jund *et al.*, 1988; Yoo *et al.*, 1992; Enjo *et al.*, 1997; Singleton, 1997; de Montigny *et al.*, 1998; Vickers *et al.*, 2000; Amillis *et al.*, 2007; Belenky *et al.*, 2008; Hamari *et al.*, 2009; Krypotou *et al.*, 2015). Fungal Fcy-like transporters have an entirely different and nonoverlapping specificity profile from that of the Fur transporters, being high-affinity H^+

J_ID: MMI Customer A_ID: MMI13559 Cadmus Art: MMI13559 Ed. Ref. No.: MMI-2016-16062.R2 Date: 19-October-16 Stage: Page: 2

symporters specific for cytosine, adenine, guanine, hypoxanthine or pyridoxine (Weber *et al*., 1990; Stolz and Vielreicher, 2003; Paluszynski *et al*., 2006; Vlanti and Diallinas, 2008; Krypotou *et al*., 2012). Plant NCS1 transporters are more similar to fungal Fur sequences but show a specificity profile overlapping that of fungal Fcy and Fur proteins; they transport adenine, guanine, allantoin and uracil (Mourad *et al*., 2012; Schein *et al*., 2013; Witz *et al*., 2012; 2014; Minton *et al*., 2016; Rapp *et al*., 2016). The two functionally known bacterial NCS1 transporters, CodB in Escherichia *coli* (Danielsen *et al*., 1992) and Mhp1 in *Microbacterium liquefaciens* (Weyand *et al*., 2008), are specific for cytosine and benzyl-hydantoin, respectively. Crystal structures of Mhp1, caught in three different conformations, are available (Shimamura *et al*., 2010; Simmons *et al*., 2014), making the NCS1 family an excellent candidate to determine how substrate binding and transport specificity is determined.

Most of our knowledge on NCS1 transporter function and specificity comes from studies in the model ascomycete *Aspergillus nidulans*. Krypotou *et al*. (2015) have shown that the Fur subfamily, in addition to major transporters specific for uracil (FurD; Amillis *et al*., 2007) or allantoin (FurA; Hamari *et al*., 2009), also includes a more promiscuous transporter specific for uric acid, allantoin and uracil (FurE), and three minor uracil transporters (FurC, FurE and FurF), whereas one additional *fur* gene encodes an intrinsically unstable protein (FurB). The identification of the function of FurE and all minor Fur transporters became possible only through their overexpression in a strain lacking all major nucleobase transporters, including deletions of FurD and FurA (Krypotou *et al*., 2015). Earlier studies have revealed that one of the five Fcy-like proteins of *A. nidulans*, FcyB, encodes a major cytosine transporter, also capable to act as a secondary purine transporter (Vlanti and Diallinas, 2008). True orthologues of FurA, FurD and FcyB have been characterized in *Saccharomyces cerevisiae* (Yoo *et al*., 1992; Jund *et al*., 1998) and the yeast pathogens *Candida albicans* (Hope *et al*., 2004; Goudela *et al*., 2006) and *Candida lusitaniae* (Gabriel *et al*., 2014), and shown to contribute to sensitivity to antifungals (5-fluorocytosine) or cytotoxic drugs (5-fluorouracil).

From studies on fungal NCS1 transporters, but also from relevant work in plants, it has become apparent that substrate specificities within the NCS1 family cannot be predicted *a priori* based on primary sequence and phylogenetic analyses, due to both divergent and convergent evolutionary plasticity. In this article we present our efforts to functionally characterize the four orphan members of the Fcy subfamily in *A. nidulans*. By employing phylogenetics, phenotypic and functional analyses of null and overexpression mutants, we establish that FcyD is a novel, moderate-affinity, low-capacity, specific adenine transporter. We also obtain evidence that FcyE is a guanine transporter. Rationally designed mutagenesis, homology modeling and substrate docking approaches in FcyD further established the critical role of specific residues in determining the substrate specificity in NCS1 transporters. Our study finally shows that two of the Fcy paralogues (FcyA and FcyC) are not related to transport of nucleobases or other established substrates of the NCS1 family, strengthening the idea that the specificity of NCS1 paralogues is significantly diversified during evolution.

Results

Phylogenetics of fungal Fcy proteins

Our primary goal was to identify the putative function of all orphan Fcy-like transporters in *A. nidulans*. We detected four previously uncharacterized Fcy-like sequences using as an *in silico* probe in standard blastp searches the FcyB protein sequence, which as described in the introduction is a well-characterized purine–cytosine/H^+ symporter (Vlanti and Diallinas, 2008; Krypotou *et al*., 2012). The Fcy-like proteins share among themselves 29.3–37.0% amino acid sequence identities (Table S1). The four novel sequences were named FcyA (AN4526), FcyC (AN7967), FcyD (AN6783) and FcyE (AN1186) (see www.aspergillusgenome.org/). None of these putative transporters could, in principle, function as major or secondary nucleobase, nucleoside or allantoin transporters, as a multiply deleted strain, lacking all currently known relevant transporters (UapA, UapC, AzgA, FcyB, FurD, CntA and FurA), shows no measurable uptake rate for these solutes. FcyA- and FcyB-like proteins are conserved in all 23 Aspergilli with known genomic sequences, FcyE- and to a less degree FcyC-like proteins are present in most Aspergilli with some evolutionary losses and some divergence in FcyC-like sequences, whereas FcyD is only present in the closely related *A. nidulans*, *Aspergillus sydowii* and *Aspergillus versicolor* (Fig. S1).

In a previous phylogenetic analysis we showed that, within the NCS1 transporter family, the fungal Fcy and Fur subfamilies are well separated by long, highly supported branches, with prokaryotic sequences lying between these two groups (Krypotou *et al*., 2015). This was also in line with an independent origin from prokaryotes. Here, we further investigated the evolution of the fungal Fcy subfamily. We extracted 102 sequences from the fungal Fcy clade and its nearest neighboring

Author Proof

ID: Suresh.jayaseelan Time: 16:45 I Path: W:/JW-MMI#160229

J_ID: MMI Customer A_ID: MMI13559 Cadmus Art: MMI13559 Ed. Ref. No.: MMI-2016-16062.R2 Date: 19-October-16 Stage: Page: 3

COLOR

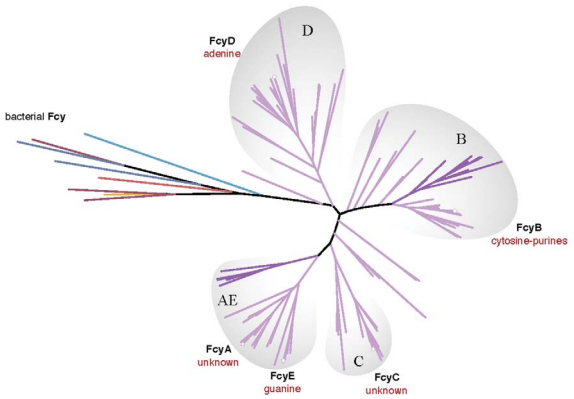

Fig. 1. Phylogenetics of fungal Fcy proteins.
Maximum Likelihood phylogenetic tree of the fungal Fcy family of transporters (102 sequences). Subgroups (AE, B, C and D) containing the fcy transporters of *A. nidulans* (FcyA-E) and substrate specificities of experimentally characterised transporters are indicated. Details on the relevant sequences are shown in Fig. S2.

prokaryotic clade and constructed a protein tree. Based on the branching patterns in the tree, and the known substrate specificities of characterized transporters, we defined four subgroups, named according to the *A. nidulans* proteins, as AE, B, C and D (Figs. 1 and S2). The AE group includes the functionally characterized Tpn1p pyridoxine transporter from *S. cerevisiae* (Stolz *et al.*, 2003). The B group includes purine–cytosine transporters from *A. nidulans* (FcyB) and yeasts (Fcy2, Fcy21 and Fcy22; Goudela *et al.*, 2006; Paluszynski *et al.*, 2006). Groups C and D have no members with characterized functions. All groups are present throughout Dikarya, despite some losses, and one of them (group B) is also present in the early diverging aquatic fungus *Gonapodya prolifera* (Fig. S2). The presence of sequences from most dikaryal main groups in all clades supports their emergence by gene duplication in the proto-Dikaryon or earlier, followed by subsequent independent losses in specific lineages.

Null mutations of orphan fcy *genes show no apparent associated phenotype*

To investigate the function of the four orphan Fcy-like transporters we carried out genetic deletions of the relative genomic orfs using standard reverse genetic approaches (see 'Experimental procedures' section). Null mutants (Δ*fcyA*, Δ*fcyC*, Δ*fcyD* and Δ*fcyE*) were compared with isogenic wild-type and Δ*fcyB* strains for growth on purines as sole nitrogen sources or on toxic concentrations of nucleobase analogues (5-fluorocytosine, 5-fluorouracil or 5-fluorouridine, 8-azaguanine, oxypurinol or purine). For comparison we also included in the test a strain carrying total genetic deletions of all known nucleobase/nucleoside/allantoin transporters (*furD*Δ *furA*Δ *fcyB*Δ *uapA*Δ *uapC*Δ *azgA*Δ *cntA*Δ), known as Δ7. Figure 2A shows that all new null mutants grow similarly to the wild-type strains in all media tested, suggesting that the corresponding genes do not encode major or minor nucleobase/nucleoside/allantoin transporters. To further investigate whether the novel Fcys act as very low-capacity functional back-ups of FcyB, we constructed and analysed relevant double or triple deleted strains. Δ*fcyB* Δ*fcyA*, Δ*fcyB* Δ*fcyC* and Δ*fcyB* Δ*fcyA* Δ*fcyE* mutants grew similar to the isogenic Δ*fcyB* mutant, while Δ*fcyA* Δ*fcyE* scored as a wild type, in all media tested (Fig. 2A, four lower panels). Thus, the biochemical and physiological functions of the orphan Fcy paralogues remained elusive.

Overexpression of orphan fcy *genes reveals that FcyD is a cryptic adenine transporter whereas FcyE contributes to 8-azaguanine sensitivity*

The absence of mutant phenotype related to null *fcy* mutants prompted us to try to identify the possible transport function of these proteins by transcriptional overexpression by the *gpdA* strong promoter (Punt *et al.*, 1990). Expression was carried out in the Δ7 mutant strain, which lacks all transporters specific for nucleobases/nucleosides/allantoin and, thus, permits the direct assessment of cryptic, very low transport activities related to these solutes (Krypotou and Diallinas, 2014). Figure 2B shows a growth test on purines as sole nitrogen sources or on toxic concentrations of nucleobase analogues (5-fluorocytosine, 5-fluorouracil, 8-azaguanine or 5-fluorouridine) of strains overexpressing FcyA, FcyB, FcyC, FcyD and FcyE (for details on strain construction see 'Experimental procedures' section), which can be compared with isogenic controls. Strains overexpressing FcyA and FcyC showed growth phenotypes similar to Δ7 (for comparison see Fig. 2A). In contrast, overexpression of FcyD and FcyE conferred strong growth on adenine or increased sensitivity to 8-azaguanine, respectively. This result classifies FcyD and FcyE as putative cryptic transporters specific for adenine and guanine, respective

Transport kinetics show that FcyD is a moderate-affinity, low-capacity, adenine transporter

We further characterized the biochemical function of FcyD by performing direct adenine or uracil uptake measurements, as described in Krypotou *et al.* (2014). Figure 3A shows that FcyD-mediated uptake of radiolabelled adenine is time dependent. Interestingly, a time-

Wiley Author Proof

ID: Suresh.jayaseelan Time: 16:45 I Path: W:/JW-MMI#160229

J_ID: MMI Customer A_ID: MMI13559 Cadmus Art: MMI13559 Ed. Ref. No.: MMI-2016-16062.R2 Date: 19-October-16 Stage: Page: 4

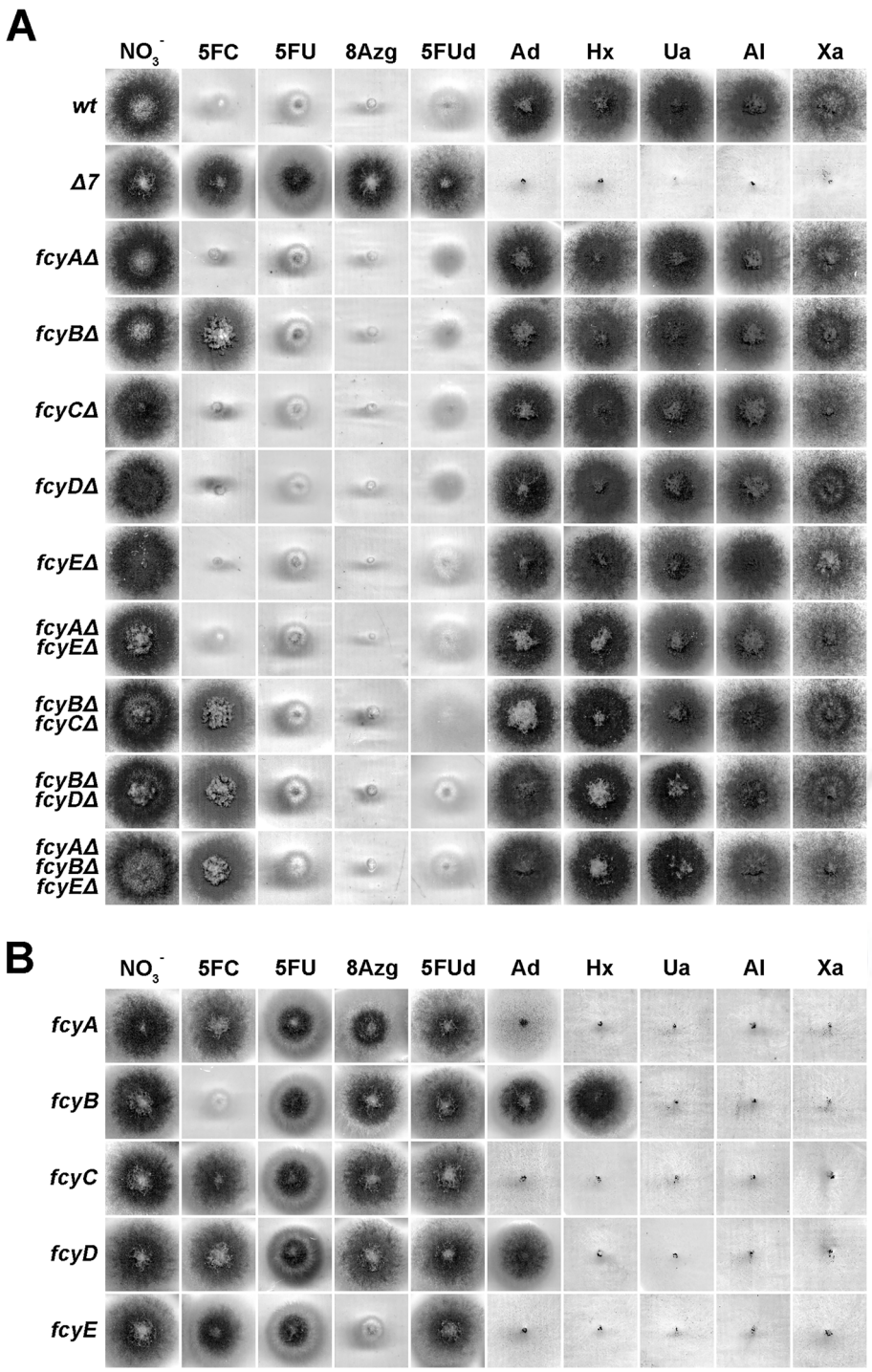

Fig. 2. Growth phenotypes of mutant strains.
A. Growth tests of all null mutants and combinations of them in a wt genetic background.
B. Overexpression of each transporter in a Δ7 genetic background, on nitrate (NO_3^-), adenine (Ad), hypoxanthine (Hx), uric acid (Ua), allantoin (Al) and xanthine (Xa) as sole nitrogen sources and in the presence of the toxic nucleobase analogues 5-fluorocytosine (5FC), 5-fluorouracil (5FU), 8-azaguanine (8Azg) and 5-fluorouridine (5Fud). Growth tests were carried out at 37°C and pH 6.8 for 48 h.

dependence continuous increase in adenine accumulation extends to nearly 20 min, unlike what has been observed for most other *A. nidulans* transporters studied so far, the transport rate of which reaches a plateau at ~2 min. No FcyD-mediated uracil (Fig. 3A) or xanthine uptake was detected for the same time period. The estimated K_m for adenine is ~131 μM (insert in Fig. 3A).

We further tested the specificity profile of FcyD by adenine competition assays in the presence of excess unlabeled purines or pyrimidines, as described in Krypotou *et al.* (2014). Figure 3B shows that FcyD is highly specific for adenine as no other purine or pyrimidine competed significantly with radiolabeled adenine uptake. Some competition (70% uptake of radiolabeled adenine

ID: Suresh.jayaseelan Time: 16:45 I Path: W:/JW-MMI#160229

J_ID: MMI Customer A_ID: MMI13559 Cadmus Art: MMI13559 Ed. Ref. No.: MMI-2016-16062.R2 Date: 19-October-16 Stage: Page: 5

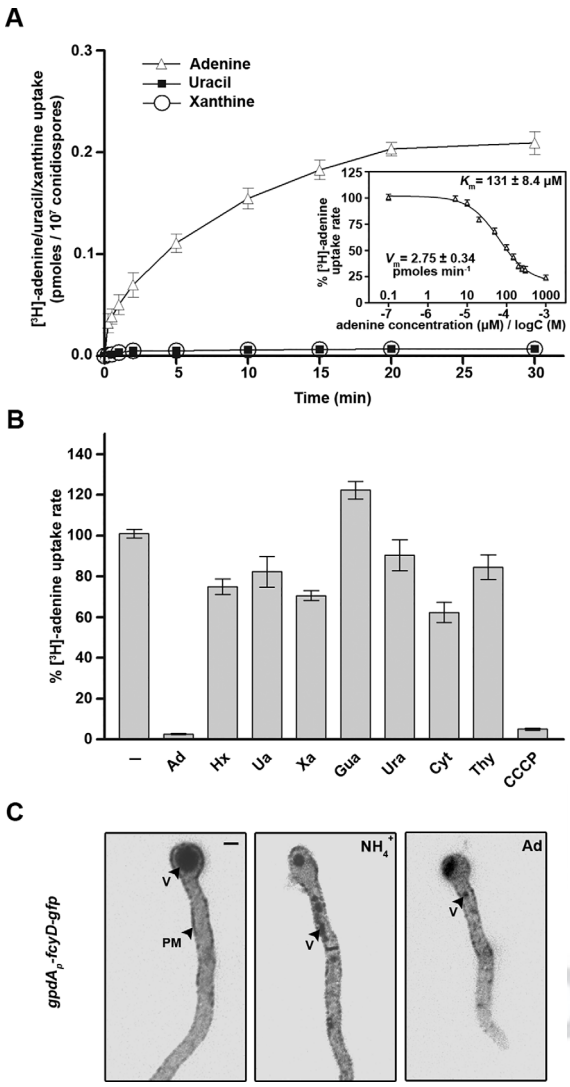

Fig. 3. FcyD is a moderate-affinity, low-capacity, adenine transporter.
A. Time course experiment using constant concentrations of [^{3}H]-adenine, uracil and xanthine. The estimated apparent K_m and V_m for adenine is shown in an insert.
B. Competition of [^{3}H]-adenine in the presence of excess 'cold' substrates (1 mM) or of the proton uncoupler CCCP. Transport rate values shown in the insert of (A) and in (B) are measured at 30 s, corresponding to the liner phase of uptake. A total of 0.1 µM of radiolabeled adenine, xanthine or uracil was used for all shown experiments.
C. Epifluorescence microscopy of over-expressed FcyD-GFP with nitrate as sole nitrogen source (–) and in the presence of ammonium (NH_4^+) and adenine (Ad). The plasma membrane (PM) and vacuoles (V) are indicated with arrowheads.

remaining) was observed with 2000-fold excess of hypoxanthine, xanthine or cytosine. Figure 3B also shows that FcyD-mediated adenine uptake is H^+-gradient dependent as it was significantly inhibited by CCCP. These results confirmed that FcyD is a moderate-affinity, low-transport capacity, highly specific adenine/H^+ symporter.

Expression of FcyD is undetectable under all conditions tested

To identify physiological conditions under which the *fcyD* gene might be expressed from its endogenous promoter, we performed a relevant Northern blot analysis using RNA extracted from wild-type mycelium grown under different physiological conditions (nitrogen source, nitrogen starvation, presence of adenine) or from conidiospores obtained at different phases of germination. However, we could not detect any signal corresponding to FcyD gene expression in any sample tested. This result is partly in line with relative transcriptomic analyses, showing that *fcyD* expression is very low in several conditions tested (complete or minimal media, nitrate or ammonium as nitrogen source, or C or N starvation). Transcriptomics also showed no expression of FcyE. In contrast, FcyA is well expressed under all conditions tested and FcyC is induced only under starvation conditions (data not shown and http://www.aspgd.org/). The significance of these observations is discussed later.

We also tested whether *fcyD* is specifically expressed in asexually or sexually differentiated cells. A strain expressing *fcyD* from its native promoter and C-terminally tagged with the *gfp* orf was constructed as described in Experimental procedures. *In vivo* epifluorescent microscopy showed that FcyD-GFP could not be detected either in conidiophores, metulae, phialidiae or in resting conidiospores (asexual structures), [illegible] cells, asci or ascospores (sexual structures) (results not shown). To test whether the absence of a fluorescent GFP signal was not due to instability or high turnover of the FcyD-GFP chimeric protein, we also expressed the FcyD-GFP chimeric construct from the $gpdA_p$ strong promoter (see 'Experimental procedures' section). Figure 3C (left panel) shows that FcyD-GFP labels the periphery of hyphal cells, as expected for a stable plasma membrane transporter, suggesting that absence of [illegible]escence when using the *fcyD* native promoter reflects the lack of sufficient transcription. Additionally, we tested whether FcyD is endocytosed and degraded in vacuoles upon the addition of ammonium or excess substrate (adenine), two standard conditions that affect nucleobase transporter turnover. Figure 3C (middle and right panels) shows that ammonium and to a less extend adenine lead to some internalization and vacuolar turnover of FcyD.

Rational mutational analysis identifies residues critical for function and specificity in FcyD

Functional characterization, mutational analysis, homology modelling and substrate docking approaches have

© 2016 John Wiley & Sons Ltd, *Molecular Microbiology,* **00**, 00–00

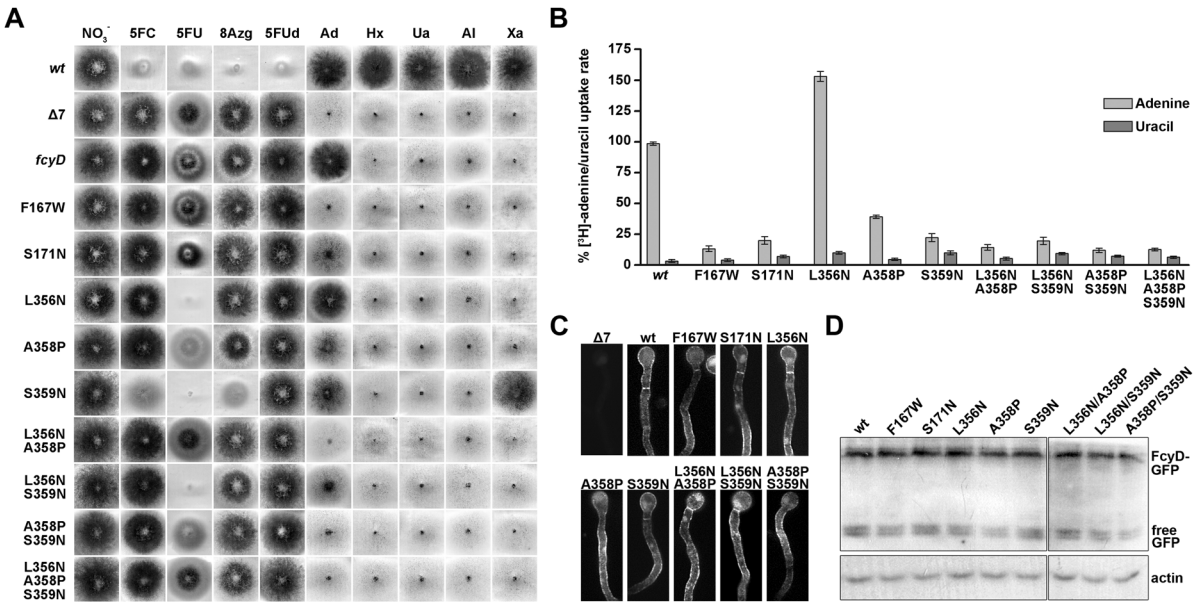

Fig. 4. Mutational analysis identifies residues critical for function and specificity.
A. Growth tests on sole nitrogen sources and nucleobase toxic analogues.
B and C. [^{3}H]-adenine initial uptake rate and epifluorescence microscopy.
D. Western blot analysis using total protein extracts of single and combinations mutants. Nitrate (NO_3^-), adenine (Ad), hypoxanthine (Hx), uric acid (Ua), allantoin (Al), xanthine (Xa), 5-fluorocytosine (5FC), 5-fluorouracil (5FU), 8-azaguanine (8Azg) and 5-fluorouridine (5Fud). For details on growth conditions see 'Experimental procedures' section.

previously identified a number of residues as putative elements of the substrate binding site in FcyB. A number of these residues were shown to be critical for substrate specificity. Comparing FcyD, which is shown herein to be highly specific for adenine, to the rather promiscuous purine–cytosine transporter FcyB, we identified specific amino acid residues differences in TMS3 and TMS8 (Fig. S3), two helices that form a part of the substrate binding cavity, which might account for the different specificity and transport kinetic profile of the two transporters. In particular, Trp159 and Asn163 (TMS3), which are critical for the transport, and Asn351, Pro353 and Asn354 (TMS8), which affect specificity, in FcyB (Krypotou *et al.*, 2012), are 'replaced' by Phe167 and Ser171 (TMS3) or Leu356, Ala358 and Ser359 (TMS8), respectively, in FcyD. Accordingly, we constructed the following mutations in FcyD mimicking FcyB: F167W, S171N, L356N, A358P, S359N, L356N/A358P, L356N/S359N, A358P/S359N and L356N/A358P/S359N. All *fcyD* alleles, expressed from the *gpdA*$_p$ promoter, were introduced to a strain lacking all transporters involved in nucleobase-related transport (Δ7) as previously described (Krypotou *et al.*, 2015) and transformants arising from plasmid single copy integration events (see 'Experimental procedures' section) were analyzed by growth tests and uptake assays.

Figure 4A shows that most single mutations made, except L356N, diminished (S171N, A358P and S359N) or abolished (F167W) the rate of apparent FcyD-mediated adenine uptake, as judged by the reduced growth rate of the corresponding mutants on adenine. In contrast, mutant L356N grew very well on adenine. Double and triple mutants showed mostly diminished (L356N/S359N) or abolished (L356N/A358P, A358P/S359N and L356N/A358P/S359N) apparent adenine transport uptake rate. Importantly, mutations L356N, S359N, L356N/S359N, and to a less degree S171N and A358P/S359N, conferred increased sensitivity to 5-FU compared to the control wild-type FcyD strain. Finally, mutant S359N also showed increased sensitivity to 5-FC and 8-azaguanine, and significant growth on xanthine. The effect of FcyD mutations was further confirmed by direct uptake assays with radiolabelled adenine. Figure 4B shows that most mutations reduced the uptake rate of FcyD for adenine uptake, whereas L356N increased the apparent transport activity of FcyD (156% of the wild-type rate). Despite the fact that L356N, S359N and L356N/S359N showed significant sensitivity to 5-FU in growth tests, these mutants did not show significant uracil uptake in transport assays, although there is some evidence for relatively increased uptake, especially in S359N, when compared to wild-type FcyD. As it will be shown later (see Fig. [redacted] and E), excess uracil competes with radiolabelled adenine uptake in S359N but not in L356N. These results suggested that the affinity for uracil or/and 5-FU for L356N

© 2016 John Wiley & Sons Ltd, *Molecular Microbiology,* **00**, 00–00

J_ID: MMI Customer A_ID: MMI13559 Cadmus Art: MMI13559 Ed. Ref. No.: MMI-2016-16062.R2 Date: 19-October-16 Stage: Page: 7

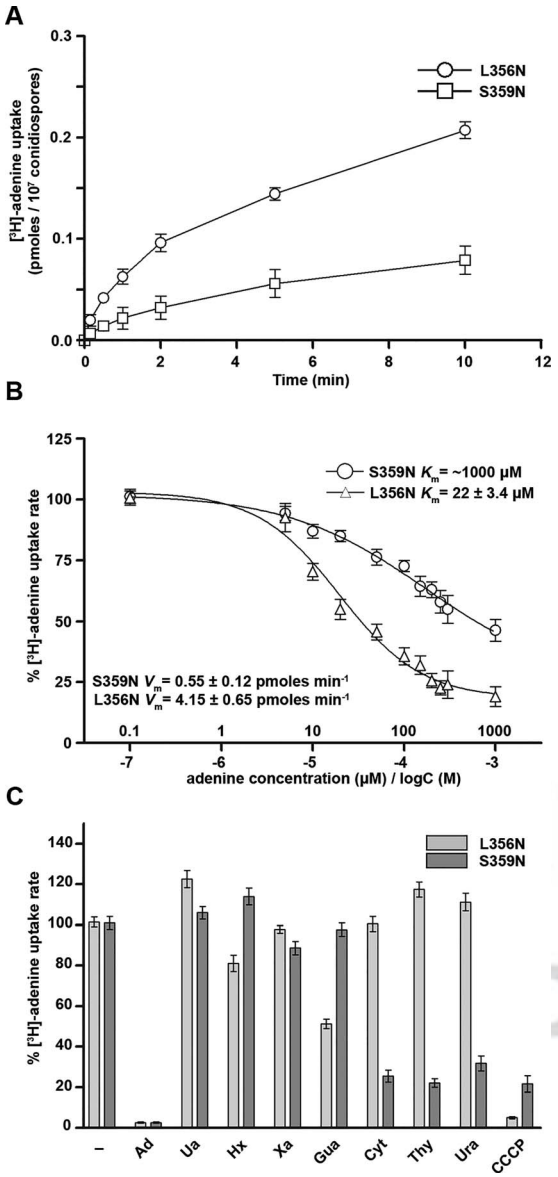

Fig. 5. Kinetic analysis of functional mutants L356N and S359N.
A. Uptake time course experiments using constant concentrations of [^{3}H]-adenine and -xanthine.
B. Estimated apparent K_m and V_m values for adenine.
C. Competition assays of [^{3}H]-adenine in the presence of excess cold substrates (1 mM) or the proton uncoupler CCCP. Transport rate values in (B) and (C) are measured at 30 s, corresponding to the liner phase of uptake. A total of 0.1 µM of radiolabeled adenine was used for all shown experiments. For more details see 'Experimental procedures' section.

might be very low (>1 mM), whereas S359N can act as a moderate affinity and transport rate uracil transporter. Overall, our results suggested that residues Phe167, Ser171 and Ala358 are critical for transport activity, Leu356 seems to affect transport kinetics (V_m and K_m values), whereas Ser359 is important for determining substrate specificity.

We constructed GFP-tagged versions of all *fcyD* alleles in order to test whether in cases of reduced apparent transport this is due to protein instability, reduced traffic to the plasma membrane or high turnover, or whether relative mutations have indeed affected transport function *per se*. Epifluorescence microscopy in Fig. 4C shows that all FcyD-GFP mutant versions, except the triple mutant L356N/A358P/S359N which shows no fluorescent signal (not shown), are properly localized in the plasma membrane, strongly suggesting that the relevant mutations affect transport function rather than protein folding and/or turnover. We also took advantage of the GFP tag to perform a western blot analysis for quantifying the protein levels of FcyD-GFP mutants (Fig. 4D). This showed that mutant FcyD protein steady state levels were not affected, except in the triple mutant L356N/A358P/S359N where the FcyD protein could not be detected, confirming that the mutations analysed do not affect the folding and/or turnover of the transporter.

Kinetic analysis of functional mutants L356N and S359N

We subsequently analysed further the transport kinetics and specificity profiles of mutants L356N and S359N, which conserved sufficient adenine transport activity for this analysis. Although mutant S359N also exhibits apparent xanthine uptake, as supported by growth tests shown in Fig. 4, we could not perform a kinetic analysis of xanthine uptake because the rate or accumulation of radiolabeled xanthine measured was too low for drawing rigorous conclusions (results not shown). Figure 5A shows a time course of uptake, which demonstrates that adenine uptake in both mutants is rather slow, increasing continuously for at least up to 10 min, similarly to wild-type FcyD-mediated transport (compare to Fig. 3A). We measured the affinity constants of the L356N and S359N mutants for adenine (Fig. 5B), as described in Krypotou *et al*. (2015). Mutation L356N increased 7.5-fold the affinity for adenine (K_m 22 µM), which might justify the increase in transport rate and growth on adenine as a nitrogen source (see Fig. 4A and B). In contrast, mutation S359N reduced 6.5-fold the affinity for adenine (K_m 1000 µM), which also seems to account for the reduced uptake rate and growth on adenine (Fig. 4A and B). We also performed relative competition assays of radiolabeled adenine transport in L356N or S359N in the presence of excess nucleobases (Fig. 5C). L356N was shown to remain specific for adenine (full competition by excess cold adenine), but also exhibiting some apparently low affinity binding ($K_i \geq 1$ mM) of guanine (~55% competition) or hypoxanthine (~22% competition). S359N-mediated radiolabelled adenine uptake was

© 2016 John Wiley & Sons Ltd, *Molecular Microbiology,* **00**, 00–00

J_ID: MMI Customer A_ID: MMI13559 Cadmus Art: MMI13559 Ed. Ref. No.: MMI-2016-16062.R2 Date: 19-October-16 Stage: Page: 8

also fully inhibited by excess cold adenine, but also showed a more promiscuous substrate recognition profile as revealed by significant inhibition by pyrimidines ($K_i \leq 1$ mM). Inhibition of S359N-mediated adenine uptake by pyrimidines was in good agreement with growth tests showing increased sensitivity to 5-FC or 5-FU (see Fig. 4A). On the other hand, the lack of significant inhibition of S359N-mediated adenine uptake by xanthine, contrasts the ability of this mutant to mediate growth on xanthine (Fig. 4A), suggesting that this purine is recognized with very low affinity or through a binding site other than that of adenine. Finally, Fig. 5C also shows that in the presence of the proton uncoupler CCCP, adenine transport is inhibited in both mutants, similarly to the wild-type (see Fig. 3C), although in mutant S359N the inhibition was somehow less efficient. These results suggest that wild-type and the analysed mutants of FcyD function as H^+/adenine symporters. This was further supported by experiments measuring adenine uptake rates at a range of pH values (4.5, 6.8 and 8.5), which showed that adenine uptake rates was relatively increased at the lowest pH, where the H^+ gradient is higher (results not shown), a standard picture obtained for several H^+ symporters studied in our lab (Meintanis *et al*., 2000 and unpublished observations).

Homology modelling and substrate docking shows that ~~a~~ Ser359 is a major residue interacting with substrates

We constructed a structural model of FcyD based on the previously made model of FcyB, which was itself produced using as a template the crystal structure of the occluded Mhp1 benzyl-hydantoin permease from *M. liquefaciens* (PDB entry: 2JLO). FcyD and FcyB share sufficient sequence similarity to sustain a solid homology model of FcyD (34% identity). The final sequence alignments used to build the FcyD model is shown in Fig. S4. The 3D structural model of FcyD is shown in Fig. S5. The model also shows the approximate adenine binding site, highlighting residues of the substrate binding site analysed genetically herein (see later). The overall topology of FcyD is similar to the previously published FcyB model (Krypotou *et al*., 2012) or other NCS1 transporters (Krypotou *et al*., 2105), consisting of two distinct domains, a compact core made of segments TMS1-10 and a C-terminal domain comprising TMS11-12. The core domain is made of the TMS1-5 and TMS6-10 inverted repeats, which are completely intertwined giving two topologically distinct subdomains made by TMSs 1, 2, 6 and 7 (bundle motif) and TMSs 3, 4, 8 and 9 (hash motif), respectively, linked with helices TMS5 and TMS10. The substrate-binding site is located in the space between the two subdomains of the core. Using this model, we addressed aspects of substrate recognition using induced fit docking (IFD) calculations (for details see 'Experimental procedures' section). Figure 6A shows the interaction of FcyD with adenine through three apparently strong H bond interactions with the side chain of Ser359 and the backbone of Gly354 and Gly267. F6

Furthermore, adenine is stabilized with π-π stacking interaction with Phe167 (Fig. 6A). No direct contact is observed with Ser171, Leu356 or Pro358, but these residues are close proximity with adenine and adenine-interacting residues so that their replacements with other amino acids are expected to affect function, as our mutational analysis showed. In particular, the L356N substitution stabilizes a hydrogen bond network among Ser359–Ans356–Asn355 (TMS8) and Ser171 (TMS3), similar to the one present on FcyB (Asn354–Asn350–Asn351–Asn163) (Krypotou *et al*., 2012), an observation that can well explain the reduced K_m for adenine (Fig. S6). Meanwhile, xanthine (Fig. 6B) shares a similar but not identical orientation in the binding pocket, interacting principally with Ser359 and the backbone of Gly354, but not with Gly267. Importantly however, xanthine also interacts strongly with the side chain of Asn90, which could trap and prevent further movement of this purine along the trajectory (Fig. 6C). Noticeably, excess xanthine competes very weakly with adenine uptake (see Fig. 3B) which suggests that xanthine and adenine translocation trajectories are only partially overlapping. In the S359N mutant, xanthine does not any more interact with Asn90 (Fig. 6D), which might account for its transport, albeit with very low-affinity and without coupling with the H^+ gradient, as our results supported.

Discussion

We have previously functionally characterized all major and secondary nucleobase/nucleoside transporters of *A. nidulans*. These belong to three structurally, functionally and evolutionary distinct protein families; the NAT (UapA, UapC and AzgA), NCS1 (FurD, FurA and FcyB) and CNT (CntA). The NCS1 family however contained 10 more paralogous proteins, classified in the Fur and Fcy subfamilies (Krypotou *et al*., 2015). We have recently characterized all six Fur paralogues and thus identified a cryptic uric acid/uracil/allantoin transporter (FurE), three very minor uracil/5-FU transporters (FurC, FurF and FurG), and a so-called proto/neo-pseudogene, encoding a polypeptide with intrinsic instability (FurB) (Krypotou *et al*., 2015). In the present work we characterised all remaining Fcy paralogues and showed that, when overexpressed, FcyD functions as a moderate-affinity adenine-specific H^+ symporter, whereas FcyE is

© 2016 John Wiley & Sons Ltd,

ID: Suresh.jayaseelan Time: 16:45 I Path: W:/JW-MMI#160229

J_ID: MMI Customer A_ID: MMI13559 Cadmus Art: MMI13559 Ed. Ref. No.: MMI-2016-16062.R2 Date: 19-October-16 Stage: Page: 9

COLOR

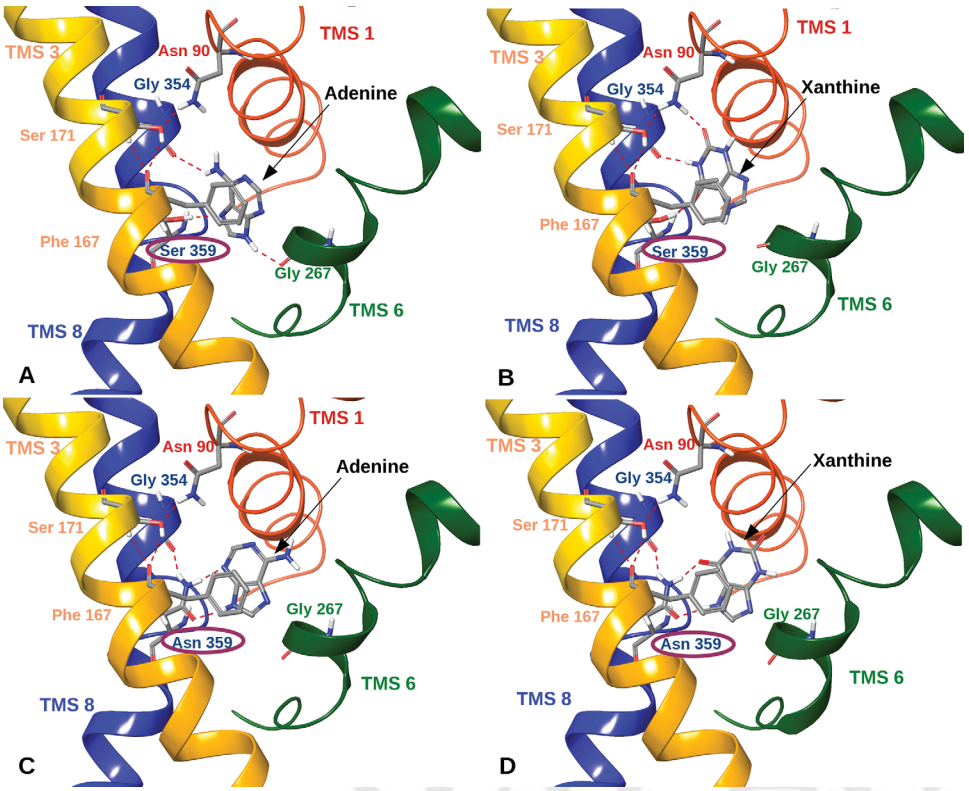

Fig. 6. Substrate docking in wt FcyD and FcyD-S359N mutant. Minimum energy structure of wild-type FcyD in complex with adenine (A) and xanthine (B) and FcyD-S359N mutant in complex with adenine (C) and xanthine (D). Hydrogen bonds are depicted with dash lines.

very probably a guanine specific transporter, as judged by its contribution to 8-azaguanine sensitivity. Unfortunately we could not characterize further FcyE due to its very low activity. Thus, this study completes the characterization of all major, secondary, minor, cryptic or putative transporters related to nucleobase/nucleoside/allantoin in *A. nidulans*. To our knowledge, this a unique case for any organism, making *A. nidulans* an ideal system to functionally express and characterise any homologous or analogous nucleobase/nucleoside transporter from other fungi, including pathogens, and possibly other eukaryotes.

The two previously orphan Fcy transporters that were biochemically and/or physiologically characterized herein as adenine (FcyD) or guanine (FcyE) transporters can be classified as cryptic transporters. This is based on the fact that they are not transcribed under standard laboratory or transcriptomics conditions, and additionally their genetic deletion is not associated with any phenotype. Furthermore, FcyD is very poorly conserved in Aspergilli. Thus, all evidence suggests that they are minor nucleobase-related transporters, which are expressed solely under specific conditions in the fungal natural habitat. On the other hand, FcyA and FcyC are well transcribed, the former under most conditions tested and the latter under N starvation conditions. In addition, these transporters are highly conserved in all Aspergilli. However, none of the two contributes to nucleobase/nucleoside/allantoin transport, strongly suggesting that they are specific for other solutes. This assumption is further supported, at least for FcyA, by the observation that this transporter has some major amino acid differences in critical residues in the presumed binding site of Fcys (e.g., a Thr instead of Asn found in FcyB and FcyE or Leu in FcyD in TMS8). We searched whether *fcy* genes are part of recognizable clusters, which might have been revealing for possible substrates, but Fcy neighbouring genes could not provide us with any clue.

Our study sheds further light in the molecular evolution of substrate specificity within the NCS1 family. We have previously identified, through a combination of genetic, biochemical and *in silico* analyses, a small number of amino acid residues that are critical for the selection, binding and transport or purines and/or pyrimidines by the major FcyB, FurD and FurE transporters. FcyB and FcyD share significant similarity (34% identity) but a major difference in respect to specificity: FcyB is a promiscuous transporter recognizing all purines, cytosine and several nucleobase analogues with high affinity, whereas FcyD is a moderate-affinity, highly specific adenine transporter. Thus, we seek to identify residues responsible for the kinetic and specificity differences in FcyB versus FcyD. Based on the structure-function

WILEY Author Proof

ID: Suresh.jayaseelan Time: 16:45 I Path: W:/JW-MMI#160229

J_ID: MMI Customer A_ID: MMI13559 Cadmus Art: MMI13559 Ed. Ref. No.: MMI-2016-16062.R2 Date: 19-October-16 Stage: Page: 10

analysis of analysis of FcyB, we designed and studied mutations in FcyD that introduced functionally critical residues present in FcyB. We thus showed that two rather variably conserved residues (Leu356 and Ser359) in transmembrane segment 8 (TMS8) are critical for transport kinetics and specificity, respectively, as expected for major residues of the substrate binding site. In particular, mutation L356N increases 7.5-fold the affinity and 2-fold the uptake rate of transporter for adenine, and also leads to low-affinity ($K_i \geq 1$ mM) recognition of guanine or hypoxanthine. Mutation S359N reduces significantly the affinity (6.5-fold) and transport uptake rate (20% of the wild type) for adenine, but drastically enlarges its specificity, so that FcyD can now transport or bind xanthine, 5-FU, 5-FC, 8-azaguanine and pyrimidines. Importantly, FcyB mutations replacing the native N354 (equivalent to S359 in FcyD) with Ala, restricts the specificity of FcyB to adenine (Krypotou *et al*., 2012). It is thus apparent that the presence of a specific Asn residue in TMS8 of Fcy-like transporters constitutes a critical evolutionary element for 'making' a promiscuous purine–pyrimidine transporter, whereas the absence of this Asn leads to increased specificity towards amino-purines.

FcyD-substrate docking models presented herein support a direct interaction of Ser359 with adenine and a critical indirect role of Leu356 in determining the affinity for adenine, through modification of architecture of the binding site. The direct role of S359N in specificity is also supported the recently revised model of Mhp1 mechanism of transport (Simmons *et al*., 2014), where an Asn residue corresponding to Ser359 of FcyD, has been shown to be the major element in direct substrate binding and transport. Interestingly, the double L356N/S359N mutant proved to have very low transport activity, suggesting that the FcyD protein cannot to sustain the simultaneous presence of the two Asn in TMS8, as in FcyB, its orthologous transporters in yeasts (Fcy2 and Fcy21) and Mhp1 (Krypotou *et al*., 2012). Similarly, FcyD could not afford a Trp residue at position 167 respectively, present in FcyB/Fcy2/Fcy21 and Mhp1. In these cases, it seems that other mutations might be needed to be introduced during evolution to 'recover' transport activity via conformational epistasis (Ortlund *et al*., 2007).

Unlike wild-type FcyD or any other Fcy-like transporter, mutant S359N also transports xanthine, despite the observation that excess cold xanthine did not compete with adenine transport. Docking studies revealed xanthine binds at similar but not identical residues in wild-type FcyD and FcyD-S359N, which might account for the observed substrate or transport differences exhibited by these proteins. This might suggest that xanthine and adenine follow partially distinct translocation trajectories of translocation in FcyD-S359N.

Experimental procedures

Sequence data/identification and phylogenetic analysis

This was essentially as described for members of the NCS1 family in Krypotou *et al*. (2015). In this study, we focused on the analysis of Fcy sequences using a reduced species sampling, we selected 81 species, covering all fungal taxonomic ranges available (61 genomes), 4 plant genomes, 20 bacterial genomes and the Mhp1 sequence from *M. liquefaciens* as the only member of the superfamily with a solved structure.

Media, strains, genetic techniques, growth conditions and A. nidulans *transformation*

Standard complete and minimal media (MM) for *A. nidulans* were used. Media and supplemented auxotrophies were at the concentrations given in http://www.fgsc.net. Nitrogen sources and analogues were used at the final concentrations: urea 5 mM, $NaNO_3$ 10 mM, purines 0.5 mM, xanthine (XA) 1 mM, 5-fluorouracil (5-FU) [redacted] M, 5-fluorouridine (5-FUd) 10 μM, 5-fluorocytosine (5-FC) 50 μM, 8-azaguanine (8-[redacted]) 0.5 mM and oxypurinol (OX) 100 μM. *Escherichia coli* was grown on Luria–Bertani medium. Media and chemical reagents were obtained from Sigma-Aldrich (Life Science Chemilab SA, Hellas) or AppliChem (Bioline Scientific SA, Hellas). Derivatives of mutant strains were made with standard genetic crossing using auxotrophic markers for heterokaryon establishment. Double or triple Δ*fcy* strains were identified by relevant PCR. *A. nidulans* transformation was performed as described previously (Koukaki *et al*., 2003). A Δ*furD::riboB* Δ*furA::riboB* Δ*fcyB::argB* Δ*azgA* Δ*uapA* Δ*uapC::AfpyrG* Δ*cntA::riboB pabaA1 pantoB100* mutant strain, named Δ7, was the recipient strain in transformations with plasmids carrying *fcy* genes or *fcyD* alleles (Krypotou and Diallinas, 2014). Δ7 lacks, due to genetic deletions, all genes encoding major transporters for purines, pyrimidines and nucleosides. Selection was based on complementation of pantothenic acid auxotrophy *pantoB100*. Transformants expressing intact *fcyD* or *fcyD–gfp* alleles, through single-copy plasmid integration events, were identified by PCR and Southern analysis. A transformant obtained with an empty vector *pantoB* and a *pabaA1* strain were used as negative and positive controls, respectively, in respect of nucleobase/nucleoside/allantoin transport. An *nkuA* DNA helicase deficient strain (TNO2A3, TNO2A7; Nayak *et al*., 2006) was the recipient strain for generating 'in locus' integrations of tagged gene fusions, or gene deletions by the *A. fumigatus* markers orotidine-5′-phosphate-decarboxylase (AF*pyrG* and Afu2g0836), or the protein required for biosynthesis of pyridoxine (AF*pyroA* and Afu5g08090), resulting in complementation of auxotrophies for uracil/uridine (*pyrG89*), or pyridoxine (*pyroA4*) respectively. Growth tests were performed at 25 or 37°C, at pH 6.8.

© 2016 John Wiley & Sons Ltd, *Molecular Microbiology,* **00**, 00–00

Author Proof

J_ID: MMI Customer A_ID: MMI13559 Cadmus Art: MMI13559 Ed. Ref. No.: MMI-2016-16062.R2 Date: 19-October-16 Stage: Page: 11

Standard nucleic acid manipulations and plasmid constructions

Genomic DNA extraction from *A. nidulans* was as described in http://www.fgsc.net. Plasmid preparation from *E. coli* strains and DNA bands were purified from agarose gels were done with the Nucleospin Plasmid kit and the Nucleospin ExtractII kit according to the manufacturer's instructions (Macherey-Nagel, Lab Supplies Scientific SA, Hellas). Southern blot analysis was performed as described in Sambrook *et al*. (1989). [^{32}P]-dCTP labeled molecules used as *fur or pantoB* specific probes were prepared using a random hexanucleotide primer kit following the supplier's instructions (Takara Bio, Lab Supplies Scientific SA, Hellas) and purified on MicroSpin™ S-200 HR columns, following the supplier's instructions (Roche Diagnostics, Hellas). Labeled [^{32}P]-dCTP (3000 Ci mmol^{-1}) was purchased from the Institute of Isotops Co. Ltd, Miklós, Hungary. Restriction enzymes were from Takara Bio (Lab Supplies Scientific SA, Hellas). Conventional PCR reactions were done with KAPA-Taq DNA polymerase (Kapa Biosystems, Lab Supplies Scientific SA, Hellas). Cloning and amplification of products were done with Kapa HiFi (Kapa Biosystems, Lab Supplies Scientific SA, Hellas).

The vector used for overexpressing *fcy* and *fcyD* alleles is a modified pGEM-T-easy vector carrying the *gpdA* promoter (~1000 bp), the *trpC* 3′ termination region, and the *pantoB* gene (Krypotou *et al*., 2015). The *fcy* ORFs were obtained from wild-type genomic DNA by PCR using appropriate primers were cloned at the SpeI-NotI sites of the vector (primer pairs 1–2, 3–4, 11–12, 13–14 and 15–16). For the overexpressed *fcyD-gfp* constructions, the relevant ORF lacking the translation stop codon was cloned together with *gfp* on the above vector (primer pairs 13–17 and 18–19). Mutations were constructed by site-directed mutagenesis (primers 26-43) according to the instructions accompanying the Quik-Change® Site-Directed Mutagenesis Kit (Stratagene) and were confirmed by sequencing (VBC-Genomics, Vienna, Austria). For the construction of *fcyD-gfp* driven under the native *fcyD* promoter, the relevant ORF-3′ regions (primer pairs 22–23 and 24–25) and the *gfp* together with AF*pyrG* (also carrying a Gly-Ala linker amplified from plasmid p1439, primer pair 20–21, Szewczyk *et al*., 2006) were first inserted in the pGEM-T vector. The fusion cassette was amplified using primers 22 and 25. The deletion cassettes of the *fcyA*Δ, *fcyC*Δ, *fcyD*Δ and *fcyE*Δ strain were amplified from purchased material from the Fungal Genetics Stock Center (http://www.fgsc.net/; Project grant GM068087, PI: J. Dunlap). For the construction of multiple *fcy*Δ mutants the *fcyB* ORF was deleted in the strains already carrying other *fcy* deletions using a cassette constructed by sequential cloning of the relevant fragments into pGEM-T vector (primer pairs 5–6, 7–8 and 9–10). Oligonucleotides used for site-directed mutagenesis, cloning or diagnostic purposes are also listed in Table S2.

Total protein extraction and western blot analysis

Cultures for total protein extraction were grown in MM supplemented with urea at 25°C for 16 h. Total protein extraction was performed as previously described (Apostolaki *et al*., 2012; Galanopoulou *et al*., 2014). Equal sample loading was estimated by Bradford assays and Coomasie staining. Total proteins (30–50 μg) were separated by SDS-PAGE (8–10%, wt/vol, polyacrylamide gel) and electroblotted (Mini PROTEAN™ Tetra Cell, BIORAD) onto PVDF membranes (Macherey-Nagel, Lab Supplies Scientific SA, Hellas) for immunodetection. The membrane was treated with 2% (wt/vol) nonfat dried milk and immunodetection was performed with a primary mouse anti-GFP monoclonal antibody (Roche Diagnostics, Hellas), a mouse anti-actin monoclonal (C4) antibody (MP Biomedicals Europe) and a secondary goat anti-mouse IgG HRP-linked antibody (Cell Signaling Technology Inc, Bioline Scientific SA, Hellas). Blots were developed by the chemiluminescent method using the LumiSensor Chemiluminescent HRP Substrate kit (Genscript USA, Lab Supplies Scientific SA, Hellas) and SuperRX Fuji medical X-Ray films (FujiFILM Europe, Lab Supplies Scientific SA, Hellas).

Kinetic analysis

The kinetic analysis was performed as recently described in detail in Krypotou and Diallinas (2014). Labelled substrates were purchased from Moravek Biochemicals, CA, USA. In more detail, [2,8-^{3}H]-adenine (20 Ci mmol^{-1}), [8-^{3}H]-xanthine (22.8 Ci mmol^{-1}) or [5,6-^{3}H]-uracil (43.9 Ci mmol^{-1}) uptake was assayed in *A. nidulans* conidiospores germinating for 3.5–4 h at 37°C, at 130–150 rpm, in liquid MM supplemented with 1% (wt/vol) glucose as a carbon source and urea or nitrate as a nitrogen source, pH 6.8. The conidiospores were collected by centrifugation and resuspended in fresh MM at a concentration of 10^7 conidiospores/100 μL. Initial velocities were measured by incubation with concentrations of 0.1 μM of labeled substrate at 37°C. The time of incubation was defined through time-course experiments and the period where each transporter showed linear increased activity was chosen respectively. Apparent $K_{m/i}$ and V_m values were obtained using labelled substrates at 0.1 μM in the presence of various concentrations (0.5–1000 μM) of nonlabelled substrates. V_m values were determined from the initial uptake rate plotted against substrate concentrations and are expressed at a concentration of 10^7 conidiospores. *V*, however, is contingent to the exact conditions of the experiment given that the absolute quantity of transporter inserted in the plasma membrane depends on growth conditions and is also under developmental control. Reactions were terminated with addition of equal volumes of ice-cold MM containing excess (1 mM) of nonradiolabelled substrate. Background counts are subtracted from the values obtained in a strain lacking the relevant transporter. The proton uncoupler carbonyl cyanide *m*-chlorophenyl hydrazone (CCCP) was used at final concentration of 30 μM. All transport assays were carried out in at least three independent experiments, with three replicates for each concentration or time point. Standard deviation was <20%. Kinetic values were analysed using the GraphPad Prism software (http://www.graphpad.com/scientific-software/prism/).

Author Proof

ID: Suresh.jayaseelan Time: 16:46 I Path: W:/JW-MMI#160229

J_ID: MMI Customer A_ID: MMI13559 Cadmus Art: MMI13559 Ed. Ref. No.: MMI-2016-16062.R2 Date: 19-October-16 Stage: Page: 12

Epifluorescence microscopy

Samples for epifluorescence microscopy were prepared as previously described (Evangelinos *et al*., 2016). In brief, germlings incubated in liquid MM supplemented with $NaNO_3$ as nitrogen source for 16–18 h at 25°C, were observed on a Zeiss Axio Observer Z1 inverted epifluorescent microscope and the resulting images were acquired with a with an AxioCam HR R3 camera using the Zen lite 2012 software. Image processing, contrast adjustment and color combining were made using the Adobe Photoshop CS4 Extended version 11.0.2 software or the ImageJ software.

Homology modeling

To construct the 3D model of FcyD (AN6783; http://www.aspgd.org/) we used as template, the theoretical structure of FcyB already published by our group (Krypotou *et al*., 2012). ClustalW was chosen for sequence alignment as implemented on Schrödigner Prime 3.7 (Prime, version 3.7, Schrödinger, LLC). The protein was additionally prepared for docking calculations using the Protein Preparation Workflow (Schrödinger Suite 2015 Protein Preparation Wizard) implemented in the Schrödinger suite and accessible from within the Maestro program (Maestro, Version 10, Schrödinger, LLC, NY, 2015). Briefly, hydrogen atoms were added, and the orientation of hydroxyl groups, Asn, Gln and the protonation state of His were optimized to maximize hydrogen bonding. Finally, the ligand–protein complex was refined with a restrained minimization performed by Impref utility that is based on the Impact molecular mechanics engine (Impact Version 6.6, Schrödinger, LLC, NY, 2015) and the OPLS2001 force field, setting a max root mean square deviation of

Induced fit docking

Molecular docking calculations were performed using the IFD protocol (Sherman *et al*., 2006a, 2006b) (Induced Fit Docking protocol 2015-2, Glide version 6.4, Prime version 3.7, Schrödinger, LLC, 2015), which is intended to circumvent the inflexible binding site and accounts for the side-chain or backbone movements, or both, upon ligand binding. The protein has been prepared using the Protein Preparation Wizard as implemented in Maestro v.10.1. In the first stage of the IFD protocol, softened-potential docking step, 20 poses per ligand were retained. In the second step, for each docking pose, a full cycle of protein refinement was performed, with Prime 3.7 (Prime, version 3.7, Schrödinger, LLC) on all residues having at least one atom within 8 Å of an atom in any of the 20 ligand poses. The Prime refinement starts with a conformational search and minimization of the side-chains of the selected residues and after convergence to a low-energy solution, an additional minimization of all selected residues (side chain and backbone) is performed with the truncated-Newton algorithm using the OPLS parameter set and a surface Generalized Born implicit solvent model. The obtained complexes are ranked according to Prime calculated energy (molecular mechanics and solvation), and those within 30 kcal mol^{-1} of the minimum energy structure are used in the last step of the process, redocking with Glide 6.4 (Glide, version 6.4, Schrödinger, LLC, 2015) using standard precision and scoring. In the final round, the ligands used in the first docking step are re-docked into each of the transporter structures retained from the refinement step. The final ranking of the complexes is done by a composite score which accounts for the transporter–ligand interaction energy (GlideScore) and solvation energies (Prime energy).

Acknowledgements

We are grateful to Emila Krypotou for her help in constructing a null mutant and Alex Pittis (Bioinformatics and Genomics Programme, CRG, Barcelona, Spain) and Claudio Scazzocchio (Imperial College) for help in performing the phylogenetic analysis. We also thank the undergraduate student Laura Piot for help in initial experiments. This study was supported by the National and Kapodistrian University of Athens.

References

Alguel, Y., Amillis, S., Leung, J., Lambrinidis, G., Capaldi, S., Scull, N.J., *et al*. (2016) Structure of eukaryotic purine/H(+) symporter UapA suggests a role for homodimerization in transport activity. *Nat Commun* **7**: 11336.

Apostolaki, A., Harispe, L., Calcagno-Pizarelli, A.M., Vangelatos, I., Sophianopoulou, V., Arst, H.N., Jr., *et al*. (2012) Aspergillus nidulans CkiA is an essential casein kinase I required for delivery of amino acid transporters to the plasma membrane. *Mol Microbiol* **84**: 530–549.

Amillis, S., Hamari, Z., Roumelioti, K., Scazzocchio, C., and Diallinas, G. (2007) Regulation of expression and kinetic modelling of substrate interactions of a uracil transporter in *Aspergillus nidulans*. *Mol Membr Biol* **24**: 206–214.

Belenky, P.A., Moga, T.G., and Brenner, C. (2008) *Saccharomyces cerevisiae* YOR071C encodes the high affinity nicotinamide riboside transporter Nrt1. *J Biol Chem* **283**: 8075–8079.

Danielsen, S., Kilstrup, M., Barilla, K., Jochimsen, B., and Neuhard, J. (1992) Characterization of the *Escherichia coli* codBA operon encoding cytosine permease and cytosine deaminase. *Mol Microbiol* **6**: 1335–1344.

de Koning, H., and Diallinas, G. (2000) Nucleobase transporters. *Mol Membr Biol* **17**: 75–94.

de Montigny, J., Straub, M.L., Wagner, R., Bach, M.L., and Chevallier, M.R. (1998) The uracil permease of *Schizosaccharomyces pombe*: a representative of a family of 10 transmembrane helix transporter proteins of yeasts. *Yeast* **14**: 1051–1059.

Diallinas, G., and Gournas, C. (2008) Structure-function relationships in the nucleobase-ascorbate transporter (NAT) family: lessons from model microbial genetic systems. *Channels (Austin)* **2**: 363–372.

Enjo, F., Nosaka, K., Ogata, M., Iwashima, A., and Nishimura, H. (1997) Isolation and characterization of a thiamin transport gene, THI10, from *Saccharomyces cerevisiae*. *J Biol Chem* **272**: 19165–19170.

© 2016 John Wiley & Sons Ltd,

ID: Suresh.jayaseelan Time: 16:46 I Path: W:/JW-MMI#160229

Evangelinos, M., Martzoukou, O., Chorozian, K., Amillis, S., and Diallinas, G. (2016) BsdA(Bsd2)-dependent vacuolar turnover of a misfolded version of the UapA transporter along the secretory pathway: prominent role of selective autophagy. *Mol Microbiol* **100**: 893–911.

Frillingos, S. (2012) Insights to the evolution of nucleobase-ascorbate transporters (NAT/NCS2 family) from the Cys-scanning analysis of xanthine permease XanQ. *Int J Biochem Mol Biol* **3**: 250–272.

Gabriel, F., Sabra, A., El-Kirat-Chatel, S., Pujol, S., Fitton-Ouhabi, V., Brèthes, D., *et al*. (2014) Deletion of the uracil permease gene confers cross-resistance to 5-fluorouracil and azoles in *Candida lusitaniae* and highlights antagonistic interaction between fluorinated nucleotides and fluconazole. *Antimicrob Agents Chemother* **58**: 4476–4485.

Galanopoulou, K., Scazzocchio, C., Galinou, M.E., Liu, W., Borbolis, F., Karachaliou, M., *et al*. (2014) Purine utilization proteins in the Eurotiales: cellular compartmentalization, phylogenetic conservation and divergence. *Fungal Genet Biol* **69**: 96–108.

Girke, C., Daumann, M., Niopek-Witz, S., and Möhlmann, T. (2014) Nucleobase and nucleoside transport and integration into plant metabolism. *Front Plant Sci* **5**: 443.

Gournas, C., Papageorgiou, I., and Diallinas, G. (2008) The nucleobase-ascorbate transporter (NAT) family: genomics, evolution, structure-function relationships and physiological role. *Mol Biosyst* **4**: 404–416.

Hamari, Z., Amillis, S., Drevet, C., Apostolaki, A., Vágvölgyi, C., Diallinas, G., and Scazzocchio, C. (2009) Convergent evolution and orphan genes in the Fur4p-like family and characterization of a general nucleoside transporter in *Aspergillus nidulans*. *Mol Microbiol* **73**: 43–57.

Hope, W.W., Tabernero, L., Denning, D.W., and Anderson, M.J. (2004) Molecular mechanisms of primary resistance to flucytosine in *Candida albicans*. *Antimicrob Agents Chemother* **48**: 4377–4386.

Jund, R., Weber, E., and Chevallier, M.R. (1988) Primary structure of the uracil transport protein of *Saccharomyces cerevisiae*. *Eur J Biochem* **171**: 417–424.

Krypotou, E., Kosti, V., Amillis, S., Myrianthopoulos, V., Mikros, E., and Diallinas, G. (2012) Modeling, substrate docking, and mutational analysis identify residues essential for the function and specificity of a eukaryotic purine-cytosine NCS1 transporter. *J Biol Chem* **287**: 36792–36803.

Krypotou, E., and Diallinas, G. (2014) Transport assays in filamentous fungi: kinetic characterization of the UapC purine transporter of Aspergillus nidulans. *Fungal Genet Biol* **63**: 1–8.

Krypotou, E., Evangelidis, T., Bobonis, J., Pittis, A.A., Gabaldón, T., Scazzocchio, C., Mikros, E., and Diallinas, G. (2015) Origin, diversification and substrate specificity in the family of NCS1/FUR transporters. *Mol Microbiol* **96**: 927–950.

Meintanis, C., Karagouni, A.D., and Diallinas, G. (2000) Amino acid residues N450 and Q449 are critical for the uptake capacity and specificity of UapA, a prototype of a nucleobase-ascorbate transporter family. *Mol Membr Biol* **17**: 47–57.

Minton, J.A., Rapp, M., Stoffer, A.J., Schultes, N.P., and Mourad, G.S. (2016) Heterologous complementation studies reveal the solute transport profiles of a two-member nucleobase cation symporter 1 (NCS1) family in Physcomitrella patens. *Plant Physiol Biochem* **100**: 12–17.

Mourad, G.S., Tippmann-Crosby, J., Hunt, K.A., Gicheru, Y., Bade, K., Mansfield, T.A., and Schultes, N.P. (2012) Genetic and molecular characterization reveals a unique nucleobase cation symporter 1 in Arabidopsis. *FEBS Lett* **586**: 1370–1378.

Nayak, T., Szewczyk, E., Oakley, C.E., Osmani, A., Ukil, L., Murray, S.L., *et al*. (2006) A versatile and efficient gene-targeting system for Aspergillus nidulans. *Genetics* **172**: 1557–1566.

Paluszynski, J.P., Klassen, R., Rohe, M., and Meinhardt, F. (2006) Various cytosine/adenine permease homologues are involved in the toxicity of 5-fluorocytosine in *Saccharomyces cerevisiae*. *Yeast* **23**: 707–715.

Pantazopoulou, A., and Diallinas, G. (2007) Fungal nucleobase transporters. *FEMS Microbiol Rev* **31**: 657–675.

Punt, P.J., Dingemanse, M.A., Kuyvenhoven, A., Soede, R.D., Pouwels, P.H., and van den Hondel, C.A. (1990) Functional elements in the promoter region of the *Aspergillus nidulans gpdA* gene encoding glyceraldehyde-3-phosphate dehydrogenase. *Gene* **93**: 101–109.

Ortlund, E.A., Bridgham, J.T., Redinbo, M.R., and Thornton, J.W. (2007) Crystal structure of an ancient protein: evolution by conformational epistasis. *Science* **317**: 1544–1548.

Rapp, M., Schein, J., Hunt, K.A., Nalam, V., Mourad, G.S., and Schultes, N.P. (2016) The solute specificity profiles of nucleobase cation symporter 1 (NCS1) from Zea mays and Setaria viridis illustrate functional flexibility. *Protoplasma* **253**: 611–623.

Sambrook, J., Fritsch, E., and Maniatis, T. (1989) *Molecular Cloning: A Laboratory Manual*. Cold Spring Harbour, NY: Cold Spring Harbour Press.

Schein, J.R., Hunt, K.A., Minton, J.A., Schultes, N.P., and Mourad, G.S. (2013) The nucleobase cation symporter 1 of *Chlamydomonas reinhardtii* and that of the evolutionarily distant *Arabidopsis thaliana* display parallel function and establish a plant-specific solute transport profile. *Plant Physiol Biochem* **70**: 52–60.

Sherman, W., Day, T., Jacobson, M.P., Friesner, R.A., and Farid, R. (2006a) Novel procedure for modelling ligand/receptor induced fit effects. *J Med Chem* **49**: 534–553.

Sherman, W., Beard, H.S., and Farid, R. (2006b) Use of an induced fit receptor structure in virtual screening. *Chem Biol Drug Des* **67**: 83–84.

Shimamura, T., Weyand, S., Beckstein, O., Rutherford, N.G., Hadden, J.M., Sharples, D., *et al*. (2010) Molecular basis of alternating access membrane transport by the sodium-hydantoin transporter Mhp1. *Science* **328**: 470–473.

Simmons, K.J., Jackson, S.M., Brueckner, F., Patching, S.G., Beckstein, O., Ivanova, E., *et al*. (2014) Molecular mechanism of ligand recognition by membrane transport protein, Mhp1. *EMBO J* **33**: 1831–1844.

Singleton, C.K. (1997) Identification and characterization of the thiamine transporter gene of *Saccharomyces cerevisiae*. *Gene* **199**: 111–121.

© 2016 John Wiley & Sons Ltd, *Molecular Microbiology,* **00**, 00–00

Stolz, J., and Vielreicher, M. (2003) Tpn1p, the plasma membrane vitamin B6 transporter of *Saccharomyces cerevisiae*. *J Biol Chem* **278**: 18990–18996.

Vickers, M.F., Yao, S.Y., Baldwin, S.A., Young, J.D., and Cass, C.E. (2000) Nucleoside transporter proteins of *Saccharomyces cerevisiae*. Demonstration of a transporter (FUI1) with high uridine selectivity in plasma membranes and a transporter (FUN26) with broad nucleoside selectivity in intracellular membranes. *J Biol Chem* **275**: 25931–25938.

Vlanti, A., and Diallinas, G. (2008) The *Aspergillus nidulans* FcyB cytosine-purine scavenger is highly expressed during germination and in reproductive compartments and is downregulated by endocytosis. *Mol Microbiol* **68**: 959–977.

Weber, E., Rodriguez, C., Chevallier, M.R., and Jund, R. (1990) The purine-cytosine permease gene of *Saccharomyces cerevisiae*: primary structure and deduced protein sequence of the FCY2 gene product. *Mol Microbiol* **4**: 585–596.

Weyand, S., Shimamura, T., Yajima, S., Suzuki, S., Mirza, O., Krusong, K., *et al*. (2008) Structure and molecular mechanism of a nucleobase-cation-symport-1 family transporter. *Science* **322**: 709–713.

Witz, S., Jung, B., Fürst, S., and Möhlmann, T. (2012) De novo pyrimidine nucleotide synthesis mainly occurs outside of plastids, but a previously undiscovered nucleobase importer provides substrates for the essential salvage pathway in Arabidopsis. *Plant Cell* **24**: 1549–1559.

Witz, S., Panwar, P., Schober, M., Deppe, J., Pasha, F.A., Lemieux, M.J., and Möhlmann, T. (2014) Structure-function relationship of a plant NCS1 member–homology modeling and mutagenesis identified residues critical for substrate specificity of PLUTO, a nucleobase transporter from Arabidopsis. *PLoS One* **9**: e91343.

Yoo, H.S., Cunningham, T.S., and Cooper, T.G. (1992) The allantoin and uracil permease gene sequences of *Saccharomyces cerevisiae* are nearly identical. *Yeast* **8**: 997–1006.

Young, J.D., Yao, S.Y., Baldwin, J.M., Cass, C.E., and Baldwin, S.A. (2013) The human concentrative and equilibrative nucleoside transporter families, SLC28 and SLC29. *Mol Aspects Med* **34**: 529–547.

Supporting information

Additional supporting information may be found in the online version of this article at the publisher's web-site.

WILEY
Author Proof

AUTHOR QUERY FORM

Dear Author,
During the preparation of your manuscript for publication, the questions listed below have arisen. Please attend to these matters and return this form with your proof.
Many thanks for your assistance.

Query References	Query	Remarks
AQ1	Please provide the end page number for the reference Alguel et al. (2016).	
AQ2	Please confirm that given names (red) and surnames/family names (green) have been identified correctly.	
AQ3	Please provide Accepted date for this manuscript.	

WILEY
Author Proof

Περίληψη

Στη παρούσα εργασία, η οποία αφορά τον μεταφορέα πυριμιδινών-πουρινών FcyB του *Aspergilllus nidulans*, μελετάται ένας αριθμός ορθολογικά σχεδιασμένων, νέων αναλόγων 3-δεαζαπουρίνης. Πιο συγκεκριμένα μελετάται η αλληλεπίδραση των ανάλογων 3-δεαζαπουρίνης με τον μεταφορέα FcyB του *Aspergillus nidulans* και ο οποίος έχει χαρακτηριστεί ως συμμεταφορέας H^+/πουρινων-κυτοσίνης. Βρέθηκε ότι ορισμένα από τα παράγωγα αναστέλλουν την πρόσληψη ραδιενεργής αδενίνης που μεσολαβείται συγκεκριμένα από τον μεταφορέα FcyB. Επιπλέον πραγματοποιήθηκαν μοριακές δομικές προσομοιώσεις του μεταφορέα FcyB μαζί με το καθένα από τα ανάλογα και τα αποτελέσματα υποδηλώνουν ότι όλες οι δραστικές ενώσεις αλληλεπιδρούν με τον μεταφορέα FcyB μέσω του σχηματισμού ενός δεσμού υδρογόνου με το αμινοξικό κατάλοιπο Asn163, παράλληλα η εισαγωγή υδρόφοβων χημικών ομάδων στην θέση 9 και N6 της 3-δεαζααδενίνης ενίσχυσε την προαναφερθείσα αναστολή.

Η έλλειψη αποτελεσματικού αντιμυκητιακού που να καταπολεμά επαρκώς το είδος παθογόνου, νηματοειδούς μύκητα *Aspergilllus fumigatus,* το οποίο αποτελεί κίνδυνο για ανοσοκατεσταλμένα άτομα, έδωσε ώθηση για την πραγματοποίηση της εργασίας αυτής, όπου σκοπός της είναι η εύρεση ενός αναλόγου πουρίνης το οποίο όχι μόνο θα μεταφέρεται με υψηλή ειδικότητα από τον μεταφορέα FcyB αλλά επιπλέον θα είναι και τοξικό και θα καταστέλλει την ανάπτυξη των κυττάρων του *Aspergilllus nidulans* αλλά και του συγγενικού του *Aspergilllus fumigatus* (στον οποίον είναι παρών όπως είναι γνωστό ο μεταφορέας FcyB και είναι ένας από τους λόγους που επιλέχθηκε αυτός ο μεταφορέας).

* Η εργασία αυτή πραγματοποιήθηκε στα πλαίσια συνεργασίας και από το άρθρο αυτό είμαι υπεύθυνη για τις εξής εικόνες: 4, 5 και τον πίνακα 1.

Bioorganic & Medicinal Chemistry 24 (2016) 5941–5952

Contents lists available at ScienceDirect

Bioorganic & Medicinal Chemistry

journal homepage: www.elsevier.com/locate/bmc

Design and synthesis of purine analogues as highly specific ligands for FcyB, a ubiquitous fungal nucleobase transporter

Nikolaos Lougiakis [a], Efthymios-Spyridon Gavriil [a], Markelos Kairis [a], Georgia Sioupouli [b], George Lambrinidis [a], Dimitra Benaki [a], Emilia Krypotou [b], Emmanuel Mikros [a], Panagiotis Marakos [a], Nicole Pouli [a,*], George Diallinas [b,*]

[a] Division of Pharmaceutical Chemistry, Department of Pharmacy, National and Kapodistrian University of Athens, Panepistimiopolis-Zografou, Athens 15771, Greece
[b] Department of Biology, National and Kapodistrian University of Athens, Panepistimiopolis, Athens 15784, Greece

ARTICLE INFO

Article history:
Received 20 June 2016
Revised 31 August 2016
Accepted 21 September 2016
Available online 22 September 2016

Keywords:
Aspergillus nidulans
Purine transporters
Structure activity relationships
Combiglide
Imidazo[4,5-*c*]pyridine
Deazaadenine

ABSTRACT

In the course of our study on fungal purine transporters, a number of new 3-deazapurine analogues have been rationally designed, based on the interaction of purine substrates with the *Aspergillus nidulans* FcyB carrier, and synthesized following an effective synthetic procedure. Certain derivatives have been found to specifically inhibit FcyB-mediated [^{3}H]-adenine uptake. Molecular simulations have been performed, suggesting that all active compounds interact with FcyB through the formation of hydrogen bonds with Asn163, while the insertion of hydrophobic fragments at position 9 and *N*6 of 3-deazaadenine enhanced the inhibition.

© 2016 Elsevier Ltd. All rights reserved.

1. Introduction

Fungal pathogens, and especially *Aspergillus fumigatus*, constitute an emerging threat due to the increasing number of immunosuppressed patients.[1,2] Most present day antifungals are rather hydrophobic compounds which enter fungal cells via non-facilitated diffusion and target enzymes involved in the synthesis of the plasma membrane or the cell wall.[3,4] The most common of such antifungals include azoles, polyenes and echinocandins. Due to the mechanism of non-specific cellular uptakes, these antifungals are associated with side effects and mediocre efficiency. In addition, resistance to these antifungals arises frequently due to genetic mechanisms activating efflux by ABC xenobiotic exporters, or the overproduction or modification of their target.[5–7] An alternative category of antifungals is exemplified by 5-fluorocytosine (5-FC). This highly efficient antifungal pyrimidine analogue is incorporated in fungal cells by specific transporters and metabolically converted to the highly cytotoxic 5-fluorouracil.[3] The apparent absence of 5-FC transporters in human cells makes this antifungal little, if not at all, cytotoxic for humans. In addition, several fungi seem to use many transporters for 5-FC uptake, so that mutation in a single gene does not confer full resistance to the drug.[8,9]

Rather surprisingly, emerging knowledge on fungal transporters has not been rationally exploited to date in relationship to the identification of novel antifungals. Ideally, a drug recognized by a fungal transporter, but not by host transporters, as is the case of 5-FC, will also have a highly targeted antifungal potential. As a step towards the rational design of novel antifungals, we study structure–function relationships in nucleobase/nucleoside transporters in *Aspergillus nidulans*, a genetically tractable fungus, where we have identified, cloned and fully characterized all 7 major transporters, catalyzing the uptake of purines, pyrimidines, nucleosides and purine analogues, namely UapA, UapC, AzgA, FurD, FurA, FcyB and CntA.[10–12] The characterization of these seven transporters has allowed the construction, through standard reverse and classical genetics, of a 'master mutant' strain named Δ7, where all seven transporter genes are deleted.[13] The genetic re-introduction of any selected nucleobase transporter gene in Δ7 allows the direct and rigorous functional assessment of the corresponding transporter in a 'clean' genetic background.[9]

In this work, we investigated whether we could rationally design, based on previously theoretical models describing purine-transporter interactions,[9,14–16] and synthesize analogues which will be recognized by a single specific nucleobase transporter of *A. nidulans*. More specifically, we wanted to test whether we can

* Corresponding authors.
E-mail addresses: pouli@pharm.uoa.gr (N. Pouli), diallina@biol.uoa.gr (G. Diallinas).

http://dx.doi.org/10.1016/j.bmc.2016.09.055
0968-0896/© 2016 Elsevier Ltd. All rights reserved.

design and synthesize purine analogues recognized solely by FcyB. We have chosen FcyB as this transporter is not only ubiquitously present in all fungi but has also very similar transport kinetics and substrate specificity with AzgA, both recognizing at the μM range and transporting efficiently all salvageable purines (adenine, guanine and hypoxanthine). Thus, being able to distinguish substrates/ligands of these two functionally similar transporters would be a rigorous test for investigating the feasibility of future efforts for rational drug design, related to specific fungal transporters. As earlier observations showed that purine analogues substituted at position 3 of the purine ring could still be recognized efficiently by FcyB,[17] 3-deazaadenine was selected as a primary compound in hit-lead campaign against FcyB. Our results show that, indeed, it is possible to identify purine analogues highly specific solely for FcyB. The importance of these findings is apparent for the future design of highly-targeted antifungals recognized by specific fungal, but not by host, transporters.

2. Results and discussion

2.1. Rational design of new 3-deaza analogues

Starting from the FcyB homology model structure previously constructed on the on the Sodium-Hydantoin Transporter Mhp1 template and validated by site mutation experiments,[15] we explored the possibilities to modify 3-deazaadenine considering the binding site of the substrate occluded structure based on the Mhp1 benzyl-hydantoin permease from *Microbacterium liquefaciens*. The resulted low energy docking poses of 3-deazaadenine within the substrate binding site of the transporter is shown in Figure 1. Two different orientations within the cavity of similar calculated interaction energy have been considered. In the first (Fig. 1A) 3-deazaadenine interacts with FcyB in a very similar way to adenine, through a bidentate H bond that is formed between Asn163 amide group and ligand sites C6-NH_2 and *N*1 (original purine numbering). In the second (Fig. 1B) 3-deazaadenine interacts with FcyB forming H bonds through C6-NH_2 and *N*7, with Asn163 as well.

According to these theoretical models two major directions can be explored as targeting regions, depicted as I and II in Figure 1 with red arrows. The first lies in the upper end of transmembrane segment 1 (TMS1) among Val84 (TMS1), Ala162, Val166 (TMS3) and Glu397 (TMS9). The second one is a hydrophobic pocket lying near Pro353 (TMS8), Trp77 (TMS1) and Tyr262 (TMS6). In order to explore those sites, 1 and 4 substituted 3-deazaadenine analogs were designed using combiglide algorithm as implemented on Schrodinger Suite 2014.

A virtual in-house library containing 100 fragments was considered for probable modifications, using 0 to 3 methylene groups as spacers, resulting 1600 virtual molecules for in silico evaluation. The resulted molecules were ranked based on GlideScore following a Virtual Screening procedure. The 40 high ranked ligands (~3 kcal/mol from global minimum) were selected as input for Induced Fit Docking. The output structures were then carefully inspected for their theoretical interactions inside the binding pocket to select the most potent substrates.

4-Methylpiperazine, 2-(dimethylamino)ethylamine and benzylamine groups appeared to be suitable modifications at position 4 of imidazopyridine to target Glu397 or Glu401 as well as more hydrophobic residues in region I. A morpholine group has been considered as alternative to piperazine to balance the hydrophobic part of the region. Isopropyl and cyclopentyl groups were best fitted within the binding pocket directed to the second targeted region II and appeared to be the most adequate moieties to be buried inside the first hydrophobic pocket near Trp77 and Ala80. Finally, the 3,5-dimethoxyphenoxy substitution was also investigated since the resulted molecule showed a different but interesting binding mode. The volume of 3,5-dimethoxyphenoxy group forces the molecule to be flipped. The *N*1-H forms hydrogen bond with Glu397, while the deazapurine core forms π–π stacking with Trp159 and the benzyl group with Trp259.

2.2. Chemistry

For the preparation of the target compounds, 2-chloropyridine (**1**, Scheme 1) was used as starting material, which underwent successively *N*-oxidation,[18] nitration and reduction of both the *N*-oxide and the nitrogroup to afford 4-amino-2-chloropyridine (**4**).[19] This compound was nitrated to result into the nitroderivatives **5** and **6**.[20] The selected 3-nitroderivative **5** was then reduced with the use of tin(II) chloride and the resulting diaminopyridine **7** was ring-closed upon reaction with triethylorthoformate to give the imidazopyridine **8**.[21] Acidic hydrolysis of **8** provided the hypoxanthine analogue **9**. On the other hand, compound **8** was treated with the suitable alkyl or arylhalide to provide the regio isomers **10a–c** and **11a–c** which were chromatographically isolated and identified using NOE spectral data (correlation peak of the protons of the substituent at position 1 with H-7, in the case

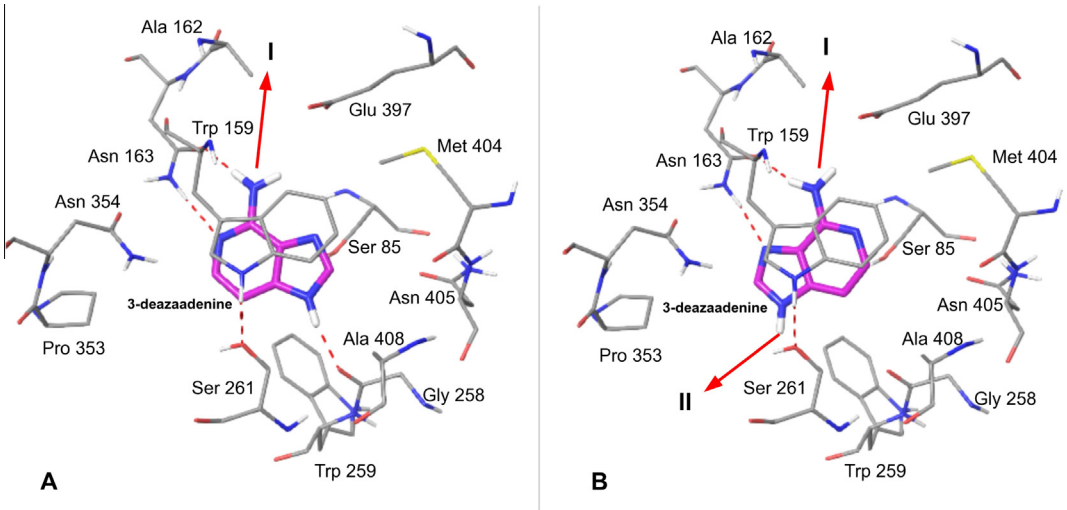

Figure 1. Global minima structures of FcyB in complex with 3-deaza-adenine (A, B). Major directions I and II for substitution are shown with red arrows.

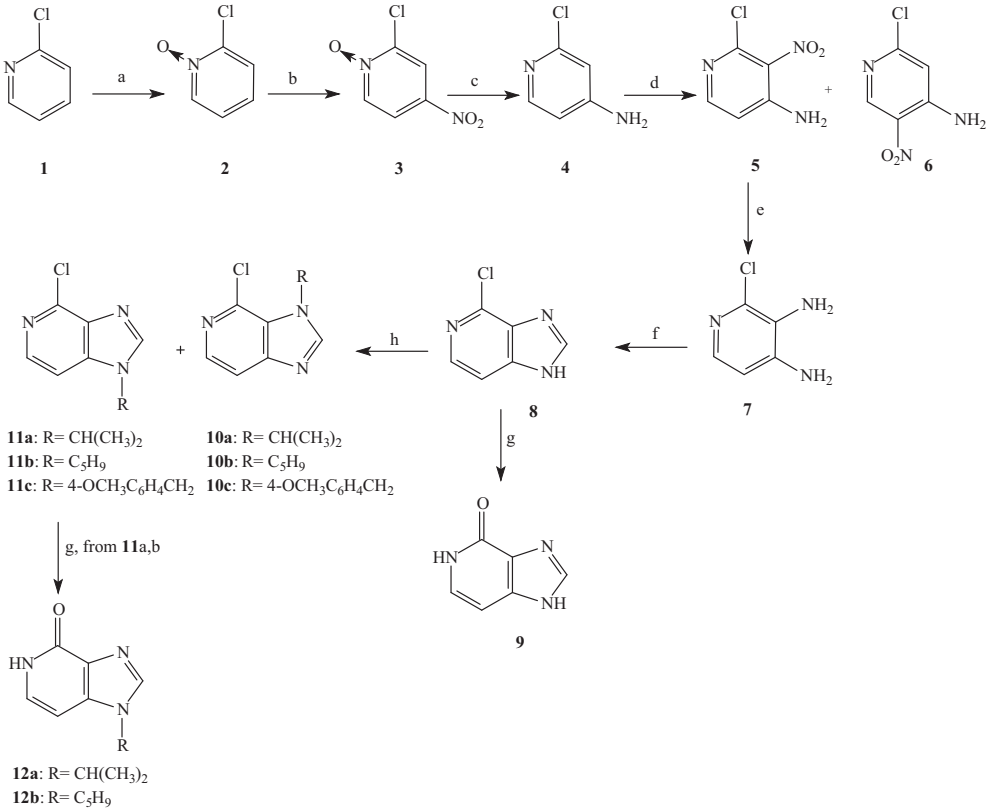

Scheme 1. Reagents and conditions: (a) *m*-CPBA, CH_2Cl_2, rt; (b) HNO_3 (fuming), H_2SO_4 (98%), 90 °C; (c) Fe, HCl (36%), EtOH, reflux; (d) (i) HNO_3 (fuming), H_2SO_4 (98%), 0 °C, (ii) H_2SO_4 (98%), 75 °C; (e) $SnCl_2{\cdot}H_2O$, HCl (36%), 50 °C; (f) triethyl orthoformate, HCl (36%), rt; (g) HCl (36%), EtOH, H_2O, reflux; (h) (i) K_2CO_3, DMF, rt, (ii) isopropyl bromide (for **10a**, **11a**) or cyclopentyl bromide (for **10b**, **11b**) or 4-methoxybenzyl chloride (for **10c**, **11c**), rt.

of compounds **11**). Then, derivatives **11a,b** were hydrolyzed to provide the corresponding imidazopyridinones **12a,b**.

Attempts to substitute the 4-chloro group of compounds **11** with suitable nucleophiles, either by refluxing compounds **11** with excess of the amine in the presence of ethanol or 2-ethoxyethanol as the solvent, or by refluxing compounds **11** in dioxane in the presence of a palladium catalyst (tris(dibenzylideneacetone)dipalladium, $Pd_2(dba)_3$) and a ligand (2-dicyclohexylphosphino-2′,4′,6′-triisopropylbiphenyl, X-Phos) in basic conditions (cesium carbonate), were not successful since they resulted in extremely low yields of the target compounds. Consequently, we have modified the synthetic methodology in order to insert the suitable substituents at an earlier stage. Thus, the nitropyridine **5** reacted with a number of primary or secondary amines as well as with a substituted phenol (Scheme 2), to provide in high yield the intermediate nitropyridines **13a**–**e**. These derivatives were reduced and the resulting diamines **14a**–**e** were cyclized without further purification to give the imidazopyridines **15a**–**e**.

From the cyclization of compound **14d**, we have also isolated the 7-amino-3-benzyl derivative **15d$_1$** (Fig. 2) in 10% yield, which has obviously resulted upon ring-closure of 2 and 3 aminogroups of **14d**.

The appropriate alkyl-group was finally inserted at position 1 of the imidazopyridines **15**, resulting into the target compounds **16a**–**k**. In the case of the 4-(3,5-dimethoxyphenoxy) derivative **15e**, the regio-isomers **17a,b** (Fig. 2), were isolated, together with the corresponding 1-substituted derivatives **16j,k**.

The 4-benzylaminoderivatives **15d**, **16h** and **16i**, were converted to the corresponding 4-aminoderivatives **18a**–**c**, upon treatment with ammonium formate in the presence of palladium on carbon as catalyst (Scheme 3).

In parallel, and in order to extract more accurate structure–activity relationships, we have also included into the biological evaluation tests adenine (**19**), as well as a number of selected 6-aminosubstituted purines (**20**–**22**, Fig. 3). Compounds **20**–**22** have been previously reported and were prepared from 6-chloropurine.[22,23] We have synthesized those derivatives in almost quantitative yield, following a slightly modified and convenient procedure, by refluxing 6-chloropurine in ethanol with two equivalents of the suitable amine.

The prepared compounds were tested, by direct in vivo transport assays, for their potential to inhibit FcyB-mediated uptake of radiolabelled hypoxanthine or adenine.

2.3. Biological studies

2.3.1. Competition at FcyB and AzgA transporter by the synthesized derivatives

The new derivatives were tested as competitive inhibitors of FcyB-mediated ^{3}H-adenine uptake. As a control for testing whether these compounds are, as expected, specific for FcyB, we also tested the same purine analogues as competitive inhibitors of AzgA-mediated ^{3}H-adenine uptake. In both cases, assays were performed in strains expressing solely the transporter studied in each case, that is, in the absence of all other functionally relative nucleobase/nucleoside-related transporters. These strains (i.e., Δ7::FcyB and Δ7::AzgA), were constructed by selecting for genetic transformants of a Δ7 mutant strain, arising from single-copy integration events of plasmids carrying either the *fcyB* or the *azgA* gene. Transformant selection was based on standard complementation of auxotrophic markers, PCR and southern analysis (for details see Section 4). In the case of FcyB, the transporter message is

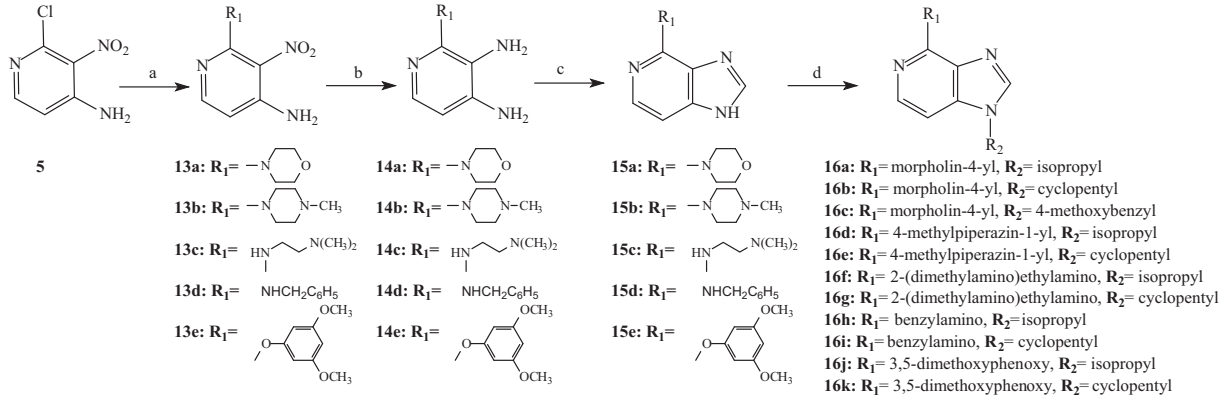

Scheme 2. Reagents and conditions: (a) amine, EtOH, reflux (for **13a–13d**) or Cs_2CO_3, 3,5-dimethoxyphenol, THF, reflux (for **13e**); (b) H_2, Pd/C, EtOH, 33–55 psi, rt; (c) triethyl orthoformate, HCl $_{(36\%)}$, rt; (d) (i) K_2CO_3, DMF, rt, (ii) isopropyl bromide (for **16a**, **16d**, **16f**, **16h**, **16j**) or cyclopentyl bromide (for **16b**, **16e**, **16g**, **16i**, **16k**) or 4-methoxybenzyl chloride (for **16c**), rt.

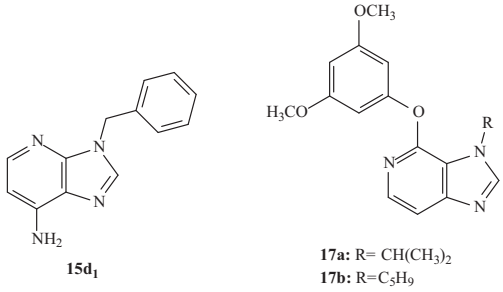

Figure 2. By-product from the cyclization of **14d** and regio-isomers of **16j–k**.

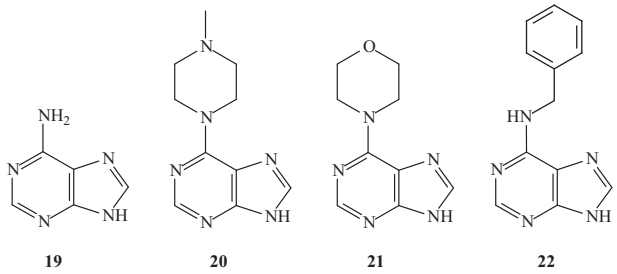

Figure 3. Adenine and aminosubstituted purines.

transcribed via the medium-strength promoter of the *uapA* gene, rather than its own native promoter, in order to achieve relatively higher protein expression levels necessary for uptake assays. The selected transformants could both grow on purines as sole nitrogen sources in the medium. As expected, Δ7::FcyB transformant was also sensitive to 5-FU, whereas the Δ7::AzgA transformant was sensitive to 8-azaguanine.

Δ7::FcyB and Δ7::AzgA strains were used to perform competitive inhibition assays of either FcyB-mediated or AzgA-mediated ^{3}H-adenine uptake, using the synthesized derivatives. Competition was carried out at 1000-fold excess inhibitors in order to identify compounds that have even low binding affinity for FcyB or AzgA. Results are shown in Figures 4 and 5 respectively. Six deazapurine analogues, **16e**, **16f**, **16g**, **16h**, **16i** and **18c** competed very efficiently FcyB-mediated ^{3}H-adenine uptake (i.e., <10% transport compared to the non-inhibited), but had no effect on AzgA-mediated ^{3}H-adenine uptake rate (compare results in Figs. 4 and 5). The same result was obtained when analogues were tested as inhibitors of FcyB-mediated or AzgA-mediated ^{3}H-hypoxanthine uptake (results not shown). These six analogues did not inhibit at all UapA, the third major purine transporter specific for xanthine or uric acid (results not shown).

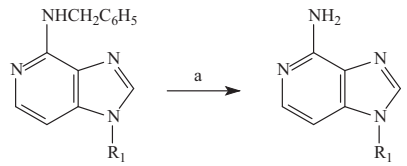

Scheme 3. Reagents and conditions: (a) $HCOONH_4$, Pd/C, MeOH, reflux.

2.3.2. Kinetic characterization of competing analogues

We estimated the K_i values, using IC_{50} measurements,[13] of the six analogues, which specifically inhibit FcyB transport. Results are shown in Table 1. All K_is were in the 5–95 μM range, with analogue **16h** showing the highest affinity binding in FcyB (5 μM).

2.4. Structure–activity relationship study

From the data presented in Figure 4 it is obvious that only the 4-amino substituted compounds possess considerable biological activity. This is confirmed by the fact that 4-chlorosubstituted derivatives **11a–c**, as well as the corresponding imidazopyridinones **9** and **12a,b** are devoid of activity. A crucial structural feature of the most potent derivatives is the simultaneous 1- and 4-substitution since compounds **16** are considerably more active than their mono-substituted counterparts **15**, with **16h** and **16i** being the most active analogues. It seems that *N*1-cyclopentyl substitution is preferable over the corresponding *N*1-isopropyl substitution. Another important finding is that among the 4-alkylamino substituted derivatives the existence of 4-NH (compounds **16f–i**) is in favor of the transporter inhibitory activity. Concerning the remaining aminosubstituted derivatives, only the piperazine analogue **16e** possesses a certain degree of activity although moderate; however, this derivative bears a *N*1-cyclopentyl moiety as well. Finally, it should be noted that although the number of derivatives is limited, our data concerning adenine and 3-deaza-adenine suggest that the 3-nitrogen is not crucial for this kind of protein ligand interaction, since the new imidazopyridines exhibited comparable activity with the purine derivatives **20–22**. However, this would request further investigation.

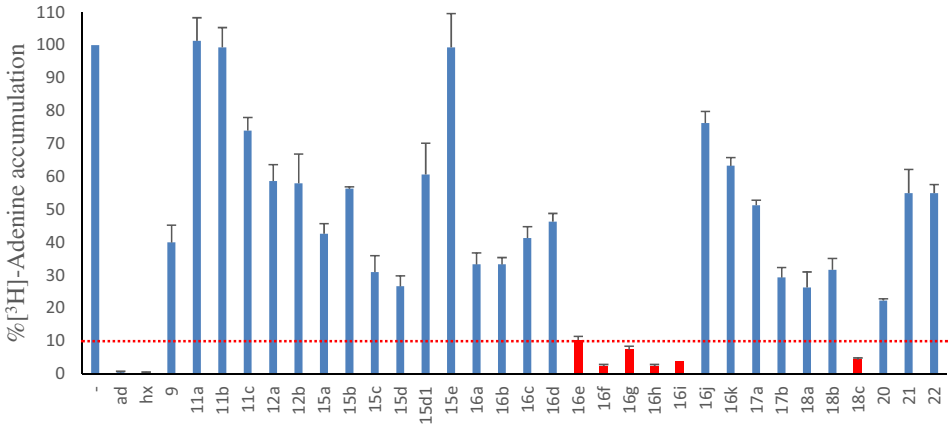

Figure 4. Competition of FcyB-mediated [^{3}H]-adenine uptake by 1000-fold excess (0.5 mM) of unlabeled purine analogues. Compounds exhibiting inhibitory activity more than 90% are depicted in red.

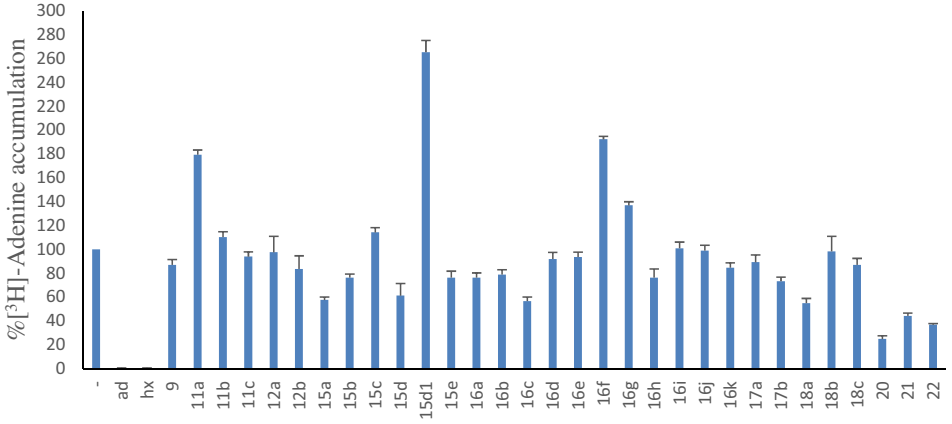

Figure 5. Competition of AzgA-mediated [^{3}H]-adenine uptake by 1000-fold excess (0.5 mM) of unlabelled purine analogues.

Table 1
Substrate binding specificity profile of FcyB

Compound	K_i (μM)
16e	38 ± 6
16f	72 ± 7
16g	95 ± 9
16h	5 ± 1
16i	21 ± 4
18c	18 ± 2

Results are averages of at least three independent experiments with three replicates for each concentration point.

2.5. Molecular modeling

Molecular simulations suggest that active compounds can interact with FcyB through residue Asn163. This residue and Pro353 were shown to be irreplaceable for FcyB-mediated transport.[15] More specifically Asn163 proved to be critical for determining the substrate binding affinity and/or specificity of FcyB, without affecting protein stability. All active compounds interact with FcyB through the formation of hydrogen bonds with Asn163. The insertion of a hydrophobic fragment at position 1 of 3-deazaadenine (**18b**, **18c**) enhanced the inhibition, especially for the cyclopentyl moiety as already mentioned. Those analogs bind at the same position as adenine and the hydrophobic fragment is placed near hydrophobic region TMS1α. (data not shown). The docking structures of the most active compounds **16h** and **16f** form a bidentate hydrogen bond (HB) via C4-NH and N3 of the ligand underlining the importance of the presence of NH at position C4 (Fig. 6). In both structures the isopropyl moiety is accommodated between Pro353, Trp77 and Tyr262 filling the space in the hydrophobic cavity. In the case of **16f** (Fig. 6B) an extra salt bridge appears possible between the tertiary amine positive charge and Glu397 carboxylate while in **16h** (Fig 6A) the phenyl group seems to exhibit hydrophobic interactions with Val84, Ala162, Val166. On all minima structures π–π stacking interactions with Trp159 and Trp259 are also very important.

3. Conclusion

In conclusion, we have designed and synthesized a number of 3-deazapurines substituted in the corresponding 6- and 9-positions of the original purine scaffold. These compounds were tested in substrate competition assays related to FcyB and AzgA transporters, both of which recognize and transport purines with high affinities at the low μM range. A number of the tested 3-deazapurines was found to be specific solely for FcyB. The K_i values of FcyB-specific substrates/ligands were determined. Given that the synthesized 3-deazapurines were designed rationally based on the interaction of purine substrates with FcyB, our results show that our approach can be used successfully to design substrates/ligands highly specific for a given nucleobase transporter. The importance of these findings is apparent for the future design of compounds recognized specifically by all fungal, but not by host, transporters.

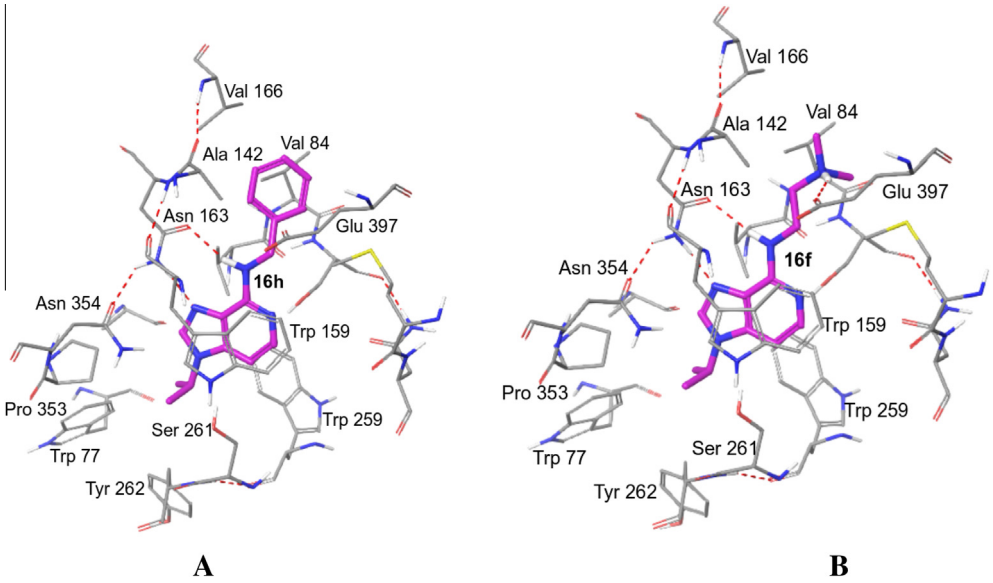

Figure 6. Minimum energy structures of FcyB in complex with compound **16h** (A) and **16f** (B). Hydrogen bonds are shown with red dashed lines.

4. Experimental section

4.1. Chemistry

4.1.1. General

Melting points were determined on a Büchi apparatus and are uncorrected. ^{1}H NMR spectra and 2D spectra were recorded on a Bruker Avance III 600 or a Bruker Avance DRX 400 instrument, whereas ^{13}C NMR spectra were recorded on a Bruker Avance III 600 or a Bruker AC 200 spectrometer in deuterated solvents and were referenced to TMS (δ scale). The signals of ^{1}H and ^{13}C spectra were unambiguously assigned by using 2D NMR techniques: ^{1}H^{1}H COSY, NOESY, HMQC, and HMBC. Mass spectra were recorded with a LTQ Orbitrap Discovery instrument, possessing an Ionmax ionization source. Flash chromatography was performed on Merck silica gel 60 (0.040–0.063 mm). Analytical thin layer chromatography (TLC) was carried out on precoated (0.25 mm) Merck silica gel F-254 plates. The purity of all the synthesized compounds was >95% as ascertained by elemental analysis. Elemental analyses were undertaken using a PerkinElmer PE 240C elemental analyzer (Norwalk, CT, U.S.) and the measured values for C, H, and N were within ±0.4% of the theoretical values.

4.1.2. General procedure for the synthesis of compounds 10a–c and 11a–c

Potassium carbonate (1.9 mmol) was added into a solution of compound **8** (1.3 mmol) in dry DMF (5 mL) under argon, and this mixture was stirred at room temperature for 20 min. Subsequently, the suitable halide (isopropyl bromide, cyclopentyl bromide, 4-methoxybenzyl chloride, 1.9 mmol) was added and the reaction was stirred at room temperature for 72 h. Then, the solvent was removed in vacuo and water was added to the residue, followed by extraction with chloroform (3 × 50 mL). The combined organic extracts were dried over sodium sulfate, filtered and the solvent was removed under reduced pressure. The 1- and 3-substituted isomers were chromatographically separated.

4.1.2.1. 4-Chloro-3-isopropyl-3*H*-imidazo[4,5-*c*]pyridine (10a) and 4-chloro-1-isopropyl-1*H*-imidazo[4,5-*c*]pyridine (11a). These derivatives were synthesized according to general procedure described above, upon reaction of compound **8** with isopropyl bromide. Purification was effected using a mixture of cyclohexane/ethyl acetate (7/3, v/v) as the eluent, to provide pure **10a** and **11a**.

Data for **10a***:* Yield 24%. White solid, mp 93 °C (Et_2O). ^{1}H NMR (600 MHz, $CDCl_3$) δ 8.16 (s, 1H, H-2), 8.14 (d, 1H, J = 5.4 Hz, H-6), 7.59 (d, 1H, J = 5.4 Hz, H-7), 5.38 (septet, 1H, J = 6.6 Hz, C*H*$(CH_3)_2$), 1.62 (d, 6H, J = 6.6 Hz, 2×CH_3). ^{13}C NMR (151 MHz, $CDCl_3$) δ 151.44 (C-7a), 143.62 (C-2), 140.88 (C-6), 133.61 (C-4), 127.91 (C-3a), 114.97 (C-7), 49.86 (*C*H$(CH_3)_2$), 23.92 (2×CH_3). HR-MS (ESI) m/z: Calcd for $C_9H_{11}ClN_3$: $[M1+H]^+$ = 196.0636, found 196.0639. Anal. Calcd for $C_9H_{10}ClN_3$: C, 55.25; H, 5.15; N, 21.48. Found: C, 55.39; H, 5.21; N, 21.38.

Data for **11a***:* Yield 76%. White solid, mp 59 °C (*n*-pentane). ^{1}H NMR (600 MHz, $CDCl_3$) δ 8.05 (d, 1H, J = 5.5 Hz, H-6), 8.02 (s, 1H, H-2), 7.27 (d, 1H, J = 5.5 Hz, H-7), 4.59 (septet, 1H, J = 6.6 Hz, C*H*$(CH_3)_2$), 1.54 (d, 6H, J = 6.6 Hz, 2×CH_3). ^{13}C NMR (151 MHz, $CDCl_3$) δ 142.48 (C-4), 141.91 (C-6), 140.70 (C-2), 139.03 (C-7a), 137.44 (C-3a), 105.61 (C-7), 48.75 (*C*H$(CH_3)_2$), 22.29 (2×CH_3). HR-MS (ESI) m/z: Calcd for $C_9H_{11}ClN_3$: $[M1+H]^+$ = 196.0636, found 196.0641. Anal. Calcd for $C_9H_{10}ClN_3$: C, 55.25; H, 5.15; N, 21.48. Found: C, 55.44; H, 5.23; N, 21.30.

4.1.2.2. 4-Chloro-3-cyclopentyl-3*H*-imidazo[4,5-*c*]pyridine (10b) and 4-chloro-1-cyclopentyl-1*H*-imidazo[4,5-*c*]pyridine (11b). These derivatives were synthesized according to general procedure described above, upon reaction of compound **8** with cyclopentyl bromide. Purification was effected using a mixture of chloroform/methanol (100/1, v/v) as the eluent, to provide pure **10b** and **11b**.

Data for **10b***:* Yield 17%. White solid, mp 77–8 °C (Et_2O). ^{1}H NMR (600 MHz, $CDCl_3$) δ 8.20 (d, 1H, J = 5.3 Hz, H-6), 8.14 (s, 1H, H-2), 7.64 (d, 1H, J = 5.3 Hz, H-7), 5.50 (m, 1H, H-1′), 2.40–2.32 (m, 2H, cyclopentyl-H), 2.05–1.97 (m, 2H, cyclopentyl-H), 1.94–1.83 (m, 4H, cyclopentyl-H). ^{13}C NMR (151 MHz, $CDCl_3$) δ 151.57 (C-4), 144.07 (C-6), 140.94 (C-2), 133.91 (C-3a), 128.46 (C-7a), 114.98 (C-7), 58.43 (C-1′), 34.06 (C-2′, C-5′), 23.77 (C-3′, C-4′). HR-MS (ESI) m/z: Calcd for $C_{11}H_{13}ClN_3$: $[M1+H]^+$ = 222.0793, found 222.0797. Anal. Calcd for $C_{11}H_{12}ClN_3$: C, 59.60; H, 5.46; N, 18.96. Found: C, 59.75; H, 5.53; N, 18.78.

Data for **11b***:* Yield 76%. White solid, mp 87–8 °C (Et_2O). ^{1}H NMR (600 MHz, $CDCl_3$) δ 8.20 (d, 1H, J = 5.6 Hz, H-6), 8.05 (s, 1H, H-2), 7.33 (d, 1H, J = 5.6 Hz, H-7), 4.74 (m, 1H, H-1′), 2.36–2.30 (m, 2H,

cyclopentyl-H), 2.06–1.99 (m, 2H, cyclopentyl-H), 1.97–1.92 (m, 2H, cyclopentyl-H), 1.89–1.83 (m, 2H, cyclopentyl-H). ^{13}C NMR (151 MHz, $CDCl_3$) δ 142.71 (C-7a), 142.49 (C-2), 140.88 (C-6), 139.66 (C-4), 137.97 (C-3a), 105.87 (C-7), 57.79 (C-1′), 32.31 (C-2′, C-5′), 23.73 (C-3′, C-4′). HR-MS (ESI) *m*/*z*: Calcd for $C_{11}H_{13}ClN_3$: $[M1+H]^+$ = 222.0793, found 222.0799. Anal. Calcd for $C_{11}H_{12}ClN_3$: C, 59.60; H, 5.46; N, 18.96. Found: C, 59.49; H, 5.40; N, 19.03.

4.1.2.3. 4-Chloro-3-(4-methoxybenzyl)-3*H*-imidazo[4,5-*c*]pyridine (10c) and 4-chloro-1-(4-methoxybenzyl)-1*H*-imidazo[4,5-*c*]pyridine (11c). These derivatives were synthesized according to general procedure described above, upon reaction of compound **8** with 4-methoxybenzyl chloride. Purification was effected using a mixture of dichloromethane/methanol (100/1, v/v) as the eluent, to provide pure **10c** (yield 18%) and **11c** (yield 45%). Compound **11c** has previously been reported.[24]

Data for **10c***:* White solid, mp 133–4 °C (Et_2O). ^{1}H NMR (600 MHz, $CDCl_3$) δ 8.25 (d, 1H, *J* = 4.5 Hz, H-6), 8.10 (s, 1H, H-2), 7.70 (d, 1H, *J* = 4.5 Hz, H-7), 7.17 (d, 2H, *J* = 8.5 Hz, H-2′, H-6′), 6.91 (d, 2H, *J* = 8.5 Hz, H-3′, H-5′), 5.70 (CH_2), 3.81 (OCH_3). ^{13}C NMR (151 MHz, $CDCl_3$) δ 160.17 (C-4′), 150.16 (C-4), 146.74 (C-2), 141.65 (C-6), 128.93 (C-2′, C-6′), 126.93 (C-3a), 126.74 (C-1′), 114.74 (C-3′, C-5′), 114.62 (C-7a), 114.57 (C-7), 55.38 (OCH_3), 50.25 (CH_2). HR-MS (ESI) *m*/*z*: Calcd for $C_{14}H_{13}ClN_3O$: $[M1+H]^+$ = 274.0742, found 274.0745. Anal. Calcd for $C_{14}H_{12}ClN_3O$: C, 61.43; H, 4.42; N, 15.35. Found: C, 61.62; H, 4.51; N, 15.17.

4.1.3. General procedure for the synthesis of compounds 12a–b

Concentrated hydrochloric acid (1 mL) was added dropwise into a solution of the corresponding chloroderivative **11** (0.25 mmol) in a mixture of ethanol (2.0 mL) and water (2.0 mL), and this reaction mixture was refluxed for 72 h. Then the organic solvent was removed in vacuo, the residue was neutralized with sodium bicarbonate and extracted with ethyl acetate. The combined organic layers were dried over sodium sulfate and the solvent was removed under reduced pressure. The residue was purified by column chromatography (silica gel) to provide pure derivatives **12a** and **12b**.

4.1.3.1. 1-Isopropyl-1,5-dihydro-4*H*-imidazo[4,5-*c*]pyridin-4-one (12a). This compound was synthesized according to general procedure described above, starting from **11a**. Purification was effected using a mixture of dichloromethane/methanol (9/1, v/v) as the eluent to provide pure **12a** as a beige solid, in 16% yield. Mp 122–3 °C (MeOH). ^{1}H NMR (400 MHz, DMSO-d_6) δ 11.15 (s, 1H, NH), 8.12 (s, 1H, H-2), 7.15 (d, *J* = 6.5 Hz, 1H, H-6), 6.62 (d, *J* = 6.5 Hz, 1H, H-7), 4.60 (septet, *J* = 6.8 Hz, 1H, *CH*(CH_3)$_2$), 1.47 (d, *J* = 6.8 Hz, 6H, CH_3). ^{13}C NMR (151 MHz, DMSO-d_6) δ 158.15 (C-4), 138.69 (C-2), 138.21 (C-7a), 131.50 (C-3a), 129.08 (C-6), 93.00 (C-7), 47.66 (*CH*(CH_3)$_2$), 22.46 (CH_3). HR-MS (ESI) *m*/*z*: Calcd for $C_9H_{12}N_3O$: $[M1+H]^+$ = 178.0975, found 178.0980. Anal. Calcd for $C_9H_{11}N_3O$: C, 61.00; H, 6.26; N, 23.71. Found: C, 60.83; H, 6.20; N, 23.89.

4.1.3.2. 1-Cyclopentyl-1,5-dihydro-4*H*-imidazo[4,5-*c*]pyridin-4-one (12b). This compound was synthesized according to general procedure described above, starting from **11b**. Purification was effected using a mixture of dichloromethane/methanol (95/5, v/v) as the eluent to provide pure **12b** as a beige solid, in 27% yield. Mp >250 °C (MeOH). ^{1}H NMR (400 MHz, DMSO-d_6) δ 11.17 (s, 1H, NH), 8.09 (s, 1H, H-2), 7.15 (d, 1H, *J* = 7.1 Hz, H-6), 6.60 (d, 1H, *J* = 7.1 Hz, H-7), 4.72 (m, 1H, H-1′), 2.17 (m, 2H, cyclopentyl-H), 1.84 (m, 4H, cyclopentyl-H), 1.69 (m, 2H, cyclopentyl-H). ^{13}C NMR (151 MHz, DMSO-d_6) δ 158.06 (C-4), 138.96 (C-2), 138.73 (C-7a), 131.58 (C-3a), 129.08 (C-6), 92.98 (C-7), 56.50 (C-1′), 32.16 (C-2′, C-5′), 23.46 (C-3′, C-4′). HR-MS (ESI) *m*/*z*: Calcd for $C_{11}H_{14}N_3O$: $[M1+H]^+$ = 204.1131, found 204.1138. Anal. Calcd for $C_{11}H_{13}N_3O$: C, 65.01; H, 6.45; N, 20.68. Found: C, 64.79; H, 6.28; N, 20.91.

4.1.4. General procedure for the synthesis of compounds 13a–d

The suitable amine (6.3 mmol) was added into a solution of compound **5** (2.9 mmol) in absolute ethanol (10 mL) and this mixture was refluxed for 2 h. Upon completion of the reaction, the organic solvent was removed under reduced pressure, water was added to the residue and the precipitate was filtered in vacuo, washed with water and air-dried, to provide the pure aminosubstituted derivatives **13a**–**d**.

4.1.4.1. 2-(Morpholin-4-yl)-3-nitropyridin-4-amine (13a). This compound was synthesized according to general procedure described above in 80% yield, upon treatment of the chloroderivative **5** with morpholine. Yellow solid, mp 131–2 °C ($CHCl_3$/Et_2O). ^{1}H NMR (600 MHz, DMSO-d_6) δ 7.67 (d, 1H, *J* = 4.5 Hz, H-6), 7.28 (br s, 2H, D_2O exch, NH_2), 6.25 (d, 1H, *J* = 4.5 Hz, H-5), 3.61 (m, 4H, H-2′, H-6′), 3.25 (m, 4H, H-3′, H-5′). ^{13}C NMR (151 MHz, DMSO-d_6) δ 154.75 (C-2), 151.11 (C-4), 148.60 (C-6), 119.37 (C-3), 103.35 (C-5), 65.89 (C-2′, C-6′), 47.91 (C-3′, C-5′). HR-MS (ESI) *m*/*z*: Calcd for $C_9H_{13}N_4O_3$: $[M1+H]^+$ = 225.0982, found 225.0979. Anal. Calcd for $C_9H_{12}N_4O_3$: C, 48.21; H, 5.39; N, 24.99. Found: C, 48.05; H, 5.30; N, 25.14.

4.1.4.2. 2-(4-Methylpiperazin-1-yl)-3-nitropyridin-4-amine (13b). This compound was synthesized according to general procedure described above in 73% yield, upon treatment of the chloroderivative **5** with *N*-methylpiperazine. Yellow solid, mp 166–7 °C (EtOAc). ^{1}H NMR (600 MHz, DMSO-d_6) δ 7.65 (d, 1H, *J* = 5 Hz, H-6), 7.24 (br s, 2H, D_2O exch, NH_2), 6.20 (d, 1H, *J* = 5 Hz, H-5) 3.25 (m, 4H, H-2′, H-6′), 2.32 (m, 4H, H-3′, H-5′), 2.18 (s, 3H, NCH_3). ^{13}C NMR (151 MHz, DMSO-d_6) δ 154.75 (C-2), 151.05 (C-4), 148.61 (C-6), 119.22 (C-3), 102.87 (C-5), 54.36 (C-3′, C-5′), 47.26 (C-2′, C-6′), 45.68 (NCH_3). HR-MS (ESI) *m*/*z*: Calcd for $C_{10}H_{16}N_5O_2$: $[M1+H]^+$ = 238.1299, found 238.1292. Anal. Calcd for $C_{10}H_{15}N_5O_2$: C, 50.62; H, 6.37; N, 29.52. Found: C, 50.82; H, 6.48; N, 29.31.

4.1.4.3. N^2-[2-(Dimethylamino)ethyl]-3-nitropyridine-2,4-diamine (13c). This compound was synthesized according to general procedure described above in 77% yield, upon treatment of the chloroderivative **5** with *N*,*N*-dimethylethylenediamine. Yellow solid, mp 120–1 °C (EtOAc/Et_2O). ^{1}H NMR (600 MHz, DMSO-d_6) δ 8.90 (t, 1H, *J* = 4.6 Hz, D_2O exch, NH), 8.09 (br s, 2H, D_2O exch, NH_2), 7.64 (d, 1H, *J* = 5.8 Hz, H-6), 6.09 (d, 1H, *J* = 5.8 Hz, H-5), 3.51 (q, 2H, *J* = 6.1 Hz, H-2′), 2.44 (t, 2H, *J* = 6.1 Hz, H-3′), 2.17 (s, 6H, 2×CH_3). ^{13}C NMR (151 MHz, DMSO-d_6) δ 154.13 (C-4), 153.41(C-2), 151.32(C-6), 116.14(C-3), 101.13(C-5), 57.50 (C-3′), 45.13 (2×CH_3), 38.87 (C-2′). HR-MS (ESI) *m*/*z*: Calcd for $C_9H_{16}N_5O_2$: $[M1+H]^+$ = 226.1299, found 226.1296. Anal. Calcd for $C_9H_{15}N_5O_2$: C, 47.99; H, 6.71; N, 31.09. Found: C, 48.26; H, 6.89; N, 30.78.

4.1.4.4. N^2-Benzyl-3-nitropyridine-2,4-diamine (13d). This compound was synthesized according to general procedure described above in 96% yield, upon treatment of the chloroderivative **5** with benzylamine. Yellow solid, mp 111–2 °C (CH_2Cl_2/*n*-pentane). ^{1}H NMR (400 MHz, DMSO-d_6) δ 9.15 (m, 1H, D_2O exch, NH), 8.12 (br s, 2H, D_2O exch, NH_2), 7.62 (d, 1H, *J* = 5.7 Hz, H-6), 7.35–7.20 (m, 5H, phenyl-H), 6.11 (d, 1H, *J* = 5.7 Hz, H-5), 4.68 (d, 2H, *J* = 5.7 Hz, CH_2). ^{13}C NMR (151 MHz, DMSO-d_6) δ 153.81 (C-2), 153.16 (C-4), 150.90 (C-6), 139.58 (C-1′), 128.19 (C-3′, C-5′), 127.14 (C-2′, C-6′), 126.59 (C-4′), 116.01 (C-3), 101.34 (C-5),

44.10 (CH_2). HR-MS (ESI) *m/z*: Calcd for $C_{12}H_{13}N_4O_2$: $[M1+H]^+$ = 245.1033, found 245.1037. Anal. Calcd for $C_{12}H_{12}N_4O_2$: C, 59.01; H, 4.95; N, 22.94. Found: C, 58.88; H, 4.89; N, 23.13.

4.1.5. 2-(3,5-Dimethoxyphenoxy)-3-nitropyridin-4-amine (13e)

3,5-Dimethoxyphenol (450 mg, 2.9 mmol) and cesium carbonate (940 mg, 2.9 mmol) were added into a solution of compound **5** (500 mg, 2.9 mmol) in tetrahydrofuran (20 mL), under argon, and this mixture was heated at 70 °C for 12 h. Upon completion of the reaction, the organic solvent was removed under reduced pressure, water was added to the residue and the precipitate was filtered in vacuo, washed with water and air-dried, to provide the pure phenoxy derivative **13e**, as a pale yellow solid in 89% yield. Mp 166–7 °C (EtOAc). ^{1}H NMR (600 MHz, DMSO-d_6) δ 7.64 (d, 1H, J = 5.7 Hz, H-6), 7.43 (br s, 2H, D_2O exch, NH_2), 6.59 (d, 1H, J = 5.7 Hz, H-5), 6.35 (s, 1H, H-4′), 6.27 (s, 2H, H-2′, H-6′), 3.71 (s, 6H, 2×OCH_3). ^{13}C NMR (151 MHz, DMSO-d_6) δ 160.89 (C-3′, C-5′), 156.49 (C-2), 154.90 (C-4), 150.77 (C-1′), 147.39 (C-6), 120.61 (C-3), 108.63 (C-5), 99.98 (C-2′, C-6′), 97.07 (C-4′), 55.43 (2×OCH_3). HR-MS (ESI) *m/z*: Calcd for $C_{13}H_{14}N_3O_5$: $[M1+H]^+$ = 292.0928, found 292.0924. Anal. Calcd for $C_{13}H_{13}N_3O_5$: C, 53.61; H, 4.50; N, 14.43. Found: C, 53.78; H, 4.55; N, 14.37.

4.1.6. General procedure for the synthesis of aminoderivatives 14a–e

A solution of the nitro derivatives **13a**–**e** (2.0 mmol) in absolute ethanol (60 mL) was hydrogenated in the presence of 10% Pd/C (90 mg) under a pressure of 33 psi for **14d** and 55 psi for the rest compounds, at room temperature for 4 h. The solution was filtered through a celite pad to remove the catalyst and the filtrate was evaporated to dryness. The diaminoderivatives **14a**–**e** were used immediately to the next step, with no further purification.

4.1.7. General procedure for the synthesis of imidazopyridines 15a–e

Concentrated hydrochloric acid (0.3 mL) was added dropwise into a suspension of the diamines **14a**–**e** (2.0 mmol) in triethyl orthoformate (5 mL), under argon, and this reaction mixture was stirred at room temperature for 14 h. The excess of triethyl orthoformate was removed under reduced pressure, the residue was dissolved in methanol, neutralized with sodium bicarbonate and then purified by column chromatography (silica gel) to provide pure derivatives **15a**–**e**.

4.1.7.1. 4-(Morpholin-4-yl)-1*H*-imidazo[4,5-*c*]pyridine (15a).

This compound was synthesized according to the general procedure described above, starting from **14a**. Purification was effected using a mixture of dichloromethane/methanol (9/1, v/v) as the eluent to provide pure **15a** as a white solid, in 92% yield. The spectroscopic data of this derivative have already been referred.[25]

4.1.7.2. 4-(4-Methylpiperazin-1-yl)-1*H*-imidazo[4,5-*c*]pyridine (15b).

This compound was synthesized according to the general procedure described above, starting from **14b**. Purification was effected using a mixture of dichloromethane/methanol (9/1, v/v) as the eluent to provide pure **15b** as a white solid, in 99% yield. Mp 234–5 °C (EtOH/Et_2O). ^{1}H NMR (400 MHz, DMSO-d_6) δ 12.61 (br s, 1H, D_2O exch, NH), 8.10 (s, 1H, H-2), 7.76 (d, 1H, J = 5.5 Hz, H-6), 6.86 (d, 1H, J = 5.5 Hz, H-7), 4.05 (m, 4H, H-2′, H-6′), 2.43 (m, 4H, H-3′, H-5′), 2.22 (s, 3H, CH_3). ^{13}C NMR (151 MHz, DMSO-d_6) δ 151.45 (C-4), 139.90 (C-6), 139.55 (C-7a), 139.23 (C-2), 128.12 (C-3a), 99.48 (C-7), 54.97 (C-3′, C-5′), 45.81 (C-2′, C-6′), 45.96 (CH_3). HR-MS (ESI) *m/z*: Calcd for $C_{11}H_{16}N_5$: $[M1+H]^+$ = 218.1400, found 218.1397. Anal. Calcd for $C_{11}H_{15}N_5$: C, 60.81; H, 6.96; N, 32.23. Found: C, 60.93; H, 7.02; N, 32.02.

4.1.7.3. 4-[(2-Dimethylamino)ethylamino]-1*H*-imidazo[4,5-*c*]pyridine (15c).

This compound was synthesized according to the general procedure described above, starting from **14c**. Purification was effected using a mixture of dichloromethane/methanol/triethylamine (8/2/0.5, v/v/v) as the eluent to provide pure **15c** as a white solid, in 60% yield. Mp 286–7 °C (MeOH/EtOAc). ^{1}H NMR (600 MHz, DMSO-d_6) δ 10.08 (br s, 1H, D_2O exch, NH-1), 8.99 (br s, 1H, D_2O exch, N*H*CH_2), 8.46 (s, 1H, H-2), 7.70 (d, 1H, J = 6.8 Hz, H-6), 7.20 (d, 1H, J = 6.8 Hz, H-7), 4.08 (m, 2H, H-2′), 3.43 (m, 2H, H-3′), 2.86 (s, 6H, 2×CH_3). ^{13}C NMR (151 MHz, DMSO-d_6) δ 147.18 (C-4), 143.56 (C-2), 139.76 (C-7a), 129.59 (C-6), 126.26 (C-3a), 100.95 (C-7), 55.52 (C-3′), 42.98 (2×CH_3), 37.71 (C-2′). HR-MS (ESI) *m/z*: Calcd for $C_{10}H_{16}N_5$: $[M1+H]^+$ = 206.1400, found 206.1393. Anal. Calcd for $C_{10}H_{15}N_5$: C, 58.51; H, 7.37; N, 34.12. Found: C, 58.68; H, 7.45; N, 33.83.

4.1.7.4. *N*-Benzyl-1*H*-imidazo[4,5-*c*]pyridin-4-amine (15d) and 3-benzyl-3*H*-imidazo[4,5-*b*]pyridin-7-amine ($15d_1$).

These compounds were obtained according to the general procedure described above, starting from **14d**. Purification was effected using a mixture of dichloromethane/methanol (100/2, v/v) as the eluent to provide pure **15d** (82% yield) and **$15d_1$** (10% yield) as white solids. The spectroscopic data of **15d** have already been referred.[26]

Data for **$15d_1$**: Mp 168–9 °C (MeOH). ^{1}H NMR (600 MHz, DMSO-d_6) δ 8.19 (s, 1H, H-2), 7.89 (d, 1H, J = 5.5 Hz, H-5), 7.34–7.25 (m, 5H, phenyl-H), 6.37 (d, 1H, J = 5.5 Hz, H-6), 6.33 (br s, D_2O exch, 2H, NH_2), 5.38 (s, 2H, CH_2). ^{13}C NMR (151 MHz, DMSO-d_6) δ 147.14 (C-3a), 146.77 (C-7), 144.77 (C-5), 140.37 (C-2), 137.64 (C-1′), 128.53 (C-2′, C-6′), 127.50 (C-4′), 127.44 (C-3′, C-5′), 122.68 (C-7a), 102.03 (C-6), 45.92 (CH_2). HR-MS (ESI) *m/z*: Calcd for $C_{13}H_{13}N_4$: $[M1+H]^+$ = 225.1135, found 225.1131. Anal. Calcd for $C_{13}H_{12}N_4$: C, 69.62; H, 5.39; N, 24.99. Found: C, 69.51; H, 5.30; N, 25.11.

4.1.7.5. 4-(3,5-Dimethoxyphenoxy)-1*H*-imidazo[4,5-*c*]pyridine (15e).

This compound was synthesized according to the general procedure described above, starting from **14e**. Purification was effected using a mixture of dichloromethane/methanol (100/2, v/v) as the eluent to provide pure **15e** as a white solid, in 77% yield. Mp 211–2 °C (MeOH). ^{1}H NMR (400 MHz, DMSO-d_6) δ 8.35 (s, 1H, H-2), 7.81 (d, 1H, J = 5.5 Hz, H-6), 7.35 (d, 1H, J = 5.5 Hz, H-7), 6.38–6.36 (m, 1H, H-4′), 6.38–6.34 (m, 2H, H-2′, H-6′), 3.73 (s, 6H, 2×OCH_3). ^{13}C NMR (151 MHz, DMSO-d_6) δ 161.08 (C-3′, C-5′), 156.00 (C-1′), 154.19 (C-4), 142.70 (C-2), 141.08 (C-7a), 138.58 (C-6), 128.52 (C-3a), 104.68 (C-7), 99.88 (C-2′, C-6′), 96.46 (C-4′), 55.50 (2×OCH_3). HR-MS (ESI) *m/z*: Calcd for $C_{14}H_{14}N_3O_3$: $[M1+H]^+$ = 272.1030, found 272.1024. Anal. Calcd for $C_{14}H_{13}N_3O_3$: C, 61.99; H, 4.83; N, 15.49. Found: C, 62.22; H, 4.96; N, 15.30.

4.1.8. General procedure for the synthesis of compounds 16a–k and 17a–b

These compounds were synthesized following an analogous synthetic procedure to the one described for the synthesis of compounds **10a**–**c** and **11a**–**c**, starting from the imidazopyridines **15a**–**e**.

4.1.8.1. 1-Isopropyl-4-(morpholin-4-yl)-1*H*-imidazo[4,5-*c*]pyridine (16a).

This compound was synthesized according to the general procedure described above, upon reaction of **15a** with isopropyl bromide. Purification was effected using a mixture of dichloromethane/methanol (100/1, v/v) as the eluent to provide pure **16a** as a white solid, in 53% yield. Mp 75–6 °C (*n*-pentane). ^{1}H NMR (600 MHz, $CDCl_3$) δ 7.93 (d, 1H, J = 5.7 Hz,H-6), 7.79 (s, 1H, H-2), 6.75 (d, 1H, J = 5.7 Hz, H-7), 4.52 (septet, 1H, J = 6.8 Hz, $CH(CH_3)_2$), 4.11 (m, 4H, H-3″, H-5″), 3.86 (m, 4H, H-2″, H-6″), 1.56 (d, 6H, J = 6.8 Hz, 2×CH_3). ^{13}C NMR (50 MHz, $CDCl_3$) δ

151.30 (C-4), 139.60 (C-7a), 138.73 (C-6), 137.26 (C-2), 128.78 (C-3a), 97.86 (C-7), 67.10 (C-2″, C-6″), 48.13 (*C*H(CH$_3$)$_2$), 47.22 (C-3″, C-5″), 22.55 (2×CH$_3$). HR-MS (ESI) *m*/*z*: Calcd for $C_{13}H_{19}N_4O$: [M1 +H]$^+$ = 247.1553, found 247.1558. Anal. Calcd for $C_{13}H_{18}N_4O$: C, 63.39; H, 7.37; N, 22.75. Found: C, 63.56; H, 7.51; N, 22.52.

4.1.8.2. 1-Cyclopentyl-4-(morpholin-4-yl)-1*H*-imidazo[4,5-*c*] pyridine (16b). This compound was synthesized according to the general procedure described above, upon reaction of **15a** with cyclopentyl bromide. Purification was effected using a mixture of dichloromethane/methanol (98/2, v/v) as the eluent to provide pure **16b** as a white solid, in 90% yield. Mp 97–8 °C (EtOAc/*n*-pentane). ^{1}H NMR (400 MHz, CDCl$_3$) δ 7.92 (d, 1H, *J* = 5.1 Hz, H-6), 7.76 (s, 1H, H-2), 6.76 (d, 1H, *J* = 5.1 Hz, H-7), 4.62 (m, 1H, H-1′), 4.20 (m, 4H, H-3″, H-5″), 3.85 (m, 4H, H-2″, H-6″), 2.27–2.17 (m, 2H, cyclopentyl-H), 2.00–1.92 (m, 2H, cyclopentyl-H), 1.91–1.84 (m, 2H, cyclopentyl-H), 1.82–1.73 (m, 2H, cyclopentyl-H). ^{13}C NMR (50 MHz, CDCl$_3$) δ 140.66 (C-4), 140.06 (C-7a), 139.92 (C-6), 137.46 (C-2), 129.04 (C-3a), 98.01 (C-7), 67.18 (C-2″, C-6″), 57.13 (C-1′), 46.96 (C-3″, C-5″), 32.36 (C-2′, C-5′), 23.81 (C-3′, C-4′). HR-MS (ESI) *m*/*z*: Calcd for $C_{15}H_{21}N_4O$: [M1 +H]$^+$ = 273.1710, found 273.1717. Anal. Calcd for $C_{15}H_{20}N_4O$: C, 66.15; H, 7.40; N, 20.57. Found: C, 66.38; H, 7.54; N, 20.31.

4.1.8.3. 1-(4-Methoxybenzyl)-4-(morpholin-4-yl)-1*H*-imidazo [4,5-*c*]pyridine (16c). This compound was synthesized according to the general procedure described above, upon reaction of **15a** with 4-methoxybenzyl chloride. Purification was effected using a mixture of dichloromethane/methanol (100/1, v/v) as the eluent to provide pure **16c** as a pale yellow oil, in 32% yield. ^{1}H NMR (400 MHz, CDCl$_3$) δ 7.87 (d, 1H, *J* = 5.7 Hz, H-6), 7.71 (s, 1H, H-2), 7.03 (d, 2H, *J* = 8.7 Hz, H-2′, H-6′), 6.80 (d, 2H, *J* = 8.7 Hz, H-3′, H-5′), 6.62 (d, 1H, *J* = 5.7 Hz, H-7), 5.13 (s, 2H, CH$_2$), 4.09 (m, 4H, H-3″, H-5″), 3.82 (m, 4H, H-2″, H-6″), 3.72 (s, 3H, OCH$_3$). ^{13}C NMR (50 MHz, CDCl$_3$) δ 159.58 (C-4′), 151.98 (C-4), 140.32 (C-6), 140.12 (C-7a), 139.66 (C-2), 128.84 (C-3a), 128.53 (C-2′, C-6′), 126.97 (C-1′), 114.41 (C-3′, C-5′), 97.63 (C-7), 67.14 (C-2″, C-6″), 55.26 (OCH$_3$), 48.37 (CH$_2$), 46.95 (C-3″, C-5″). HR-MS (ESI) *m*/*z*: Calcd for $C_{18}H_{21}N_4O_2$: [M1+H]$^+$ = 325.1659, found 325.1664. Anal. Calcd for $C_{18}H_{20}N_4O_2$: C, 66.65; H, 6.21; N, 17.27. Found: C, 66.39; H, 6.04; N, 17.50.

4.1.8.4. 1-Isopropyl-4-(4-methylpiperazin-1-yl)-1*H*-imidazo [4,5-*c*]pyridine (16d). This compound was synthesized according to the general procedure described above, upon reaction of **15b** with isopropyl bromide. Purification was effected using a mixture of dichloromethane/methanol (9/1, v/v) as the eluent to provide pure **16d** as a white solid, in 84% yield. Mp 168–9 °C (CH$_2$-Cl$_2$). ^{1}H NMR (600 MHz, CDCl$_3$) δ 7.86 (d, 1H, *J* = 5.7 Hz, H-6), 7.73 (s, 1H, H-2), 6.66 (d, 1H, *J* = 5.7 Hz, H-7), 4.44 (septet, 1H, *J* = 6.8 Hz, C*H*(CH$_3$)$_2$), 4.13 (m, 4H, H-2″, H-6″), 2.54 (m, 4H, H-3″, H-5″), 2.28 (s, 3H, NCH$_3$), 1.49 (d, 6H, *J* = 6.8 Hz, 2×CH$_3$). ^{13}C NMR (151 MHz, CDCl$_3$) δ 152.09 (C-4), 140.13 (C-6), 139.36 (C-7a), 136.69 (C-2), 128.91 (C-3a), 97.44 (C-7), 55.23 (C-3″, C-5″), 47.90 (*C*H(CH$_3$)$_2$), 46.10 (NCH$_3$, C-2″, C-6″), 22.50 (2×CH$_3$). HR-MS (ESI) *m*/*z*: Calcd for $C_{14}H_{22}N_5$: [M1+H]$^+$ = 260.1870, found 260.1876. Anal. Calcd for $C_{14}H_{21}N_5$: C, 64.84; H, 8.16; N, 27.00. Found: C, 64.64; H, 8.11; N, 27.21.

4.1.8.5. 1-Cyclopentyl-4-(4-methylpiperazin-1-yl)-1*H*-imidazo [4,5-*c*]pyridine (16e). This compound was synthesized according to the general procedure described above, upon reaction of **15b** with cyclopentyl bromide. Purification was effected using a mixture of dichloromethane/methanol (9/1, v/v) as the eluent to provide pure **16e** as a white solid, in 45% yield. Mp 192–3 °C (CHCl$_3$/Et$_2$O). ^{1}H NMR (600 MHz, CDCl$_3$) δ 7.90 (d, 1H, *J* = 5.7 Hz, H-6), 7.75 (s, 1H, H-2), 6.73 (d, 1H, *J* = 5.7 Hz, H-7), 4.61 (m, 1H, H-1′), 4.17 (m, 4H, H-2″, H-6″), 2.61 (m, 4H, H-3″, H-5″), 2.35 (s, 3H, NCH$_3$), 2.25–2.15 (m, 2H, cyclopentyl-H), 1.98–1.91 (m, 2H, cyclopentyl-H), 1.89–1.82 (m, 2H, cyclopentyl-H), 1.81–1.73 (m, 2H, cyclopentyl-H). ^{13}C NMR (151 MHz, CDCl$_3$) δ 152.08 (C-4), 140.17 (C-6), 139.97 (C-7a), 137.43 (C-2), 129.07 (C-3a), 97.86 (C-7), 57.23 (C-1′), 55.27 (C-3″, C-5″), 46.12 (NCH$_3$, C-2″, C-6″), 32.37 (C-2′, C-5′), 23.91 (C-3′, C-4′). HR-MS (ESI) *m*/*z*: Calcd for $C_{16}H_{24}N_5$: [M1+H]$^+$ = 286.2026, found 286.2032. Anal. Calcd for $C_{16}H_{23}N_5$: C, 67.34; H, 8.12; N, 24.54. Found: C, 67.03; H, 8.02; N, 24.88.

4.1.8.6. 4-[2-(Dimethylamino)ethylamino]-1-isopropyl-1*H*-imidazo[4,5-*c*]pyridine (16f). This compound was synthesized according to the general procedure described above, upon reaction of **15c** with isopropyl bromide. Purification was effected using a mixture of dichloromethane/methanol/triethylamine (85/15/5, v/v/v) as the eluent to provide pure **16f** as an orange colored oil, in 84% yield. ^{1}H NMR (600 MHz, CDCl$_3$) δ 7.86 (s, 1H, H-2), 7.85 (1H, *J* = 6.1 Hz, H-6), 6.71 (d, 1H, *J* = 6.1 Hz, H-7), 6.01 (br s, 1H, D$_2$O exch, NH), 4.54 (septet, 1H, *J* = 6.7 Hz, C*H*(CH$_3$)$_2$), 3.89 (t, 2H, *J* = 6.1 Hz, H-2′), 2.97 (t, 2H, *J* = 6.1 Hz, H-3′), 2.55 (s, 6H, N(CH$_3$)$_2$), 1.58 (d, 6H, *J* = 6.7 Hz, 2×CH$_3$). ^{13}C NMR (151 MHz, CDCl$_3$) δ 151.10 (C-4), 139.23 (C-6), 138.58 (C-2), 137.69 (C-3a), 127.79 (C-7a), 97.24 (C-7), 58.01(C-3′), 48.49 (*C*H(CH$_3$)$_2$), 44.55 (N(CH$_3$)$_2$), 38.07 (C-2′), 22.71 (2×CH$_3$). HR-MS (ESI) *m*/*z*: Calcd for $C_{13}H_{22}N_5$: [M1+H]$^+$ = 248.1870, found 248.1874. Anal. Calcd for $C_{13}H_{21}N_5$: C, 63.13; H, 8.56; N, 28.31. Found: C, 63.31; H, 8.63; N, 28.02.

4.1.8.7. 1-Cyclopentyl-4-[2-(dimethylamino)ethylamino]-1*H*-imidazo[4,5-*c*]pyridine (16g). This compound was synthesized according to the general procedure described above, upon reaction of **15c** with cyclopentyl bromide. Purification was effected using a mixture of dichloromethane/methanol (85/15, v/v) as the eluent to provide pure **16g** as an orange colored oil, in 81% yield. ^{1}H NMR (400 MHz, CD$_3$OD) δ 8.26 (s, 1H, H-2), 7.85 (d, 1H, *J* = 6.3 Hz, H-6), 7.10 (d, 1H, *J* = 6.3 Hz, H-7), 4.87 (m, 1H, H-1′), 3.97 (t, 2H, *J* = 5.3 Hz, H-2″), 3.46 (t, 2H, *J* = 5.3 Hz, H-3″), 3.01 (s, 6H, 2×CH$_3$), 2.34–2.26 (m, 2H, cyclopentyl-H), 2.03–1.96 (m, 2H, cyclopentyl-H), 1.96–1.90 (m, 2H, cyclopentyl-H), 1.86–1.79 (m, 2H, cyclopentyl-H). ^{13}C NMR (151 MHz, CD$_3$OD) δ 151.79 (C-4), 142.65 (C-2), 140.54 (C-7a), 137.73 (C-6), 128.62 (C-3a), 100.37 (C-7), 60.36 (C-3″), 59.04(C-1′), 44.06 (N(CH$_3$)$_2$), 39.29 (C-2″), 33.49 (C-2′, C-5′), 25.00 (C-3′, C-4′). HR-MS (ESI) *m*/*z*: Calcd for $C_{15}H_{24}N_5$: [M1+H]$^+$ = 274.2026, found 274.2030. Anal. Calcd for $C_{15}H_{23}N_5$: C, 65.90; H, 8.48; N, 25.62. Found: C, 66.06; H, 8.53; N, 25.39.

4.1.8.8. *N*-Benzyl-1-isopropyl-1*H*-imidazo[4,5-*c*]pyridin-4-amine (16h). This compound was synthesized according to the general procedure described above, upon reaction of **15d** with isopropyl bromide. Purification was effected using a mixture of dichloromethane/methanol (100/2, v/v) as the eluent to provide pure **16h** as a pale yellow oil, in 86% yield. ^{1}H NMR (600 MHz, CDCl$_3$) δ 7.91 (d, 1H, *J* = 5.9 Hz, H-6), 7.75 (s, 1H, H-2), 7.41 (d, 2H, *J* = 7.2 Hz, H-2′, H-6′), 7.31 (t, 2H, *J* = 7.2 Hz, H-3′, H-5′), 7.24 (t, 1H, *J* = 7.2 Hz, H-4′), 6.70 (d, 1H, *J* = 5.9 Hz, H-7), 5.90 (br s, 1H, D$_2$O exch, NH), 4.83 (d, 2H, *J* = 5.6 Hz, CH$_2$), 4.53 (septet, 1H, *J* = 6.7 Hz,CH(CH$_3$)$_2$), 1.58 (d, 6H, *J* = 6.7 Hz, 2×CH$_3$). ^{13}C NMR (151 MHz, CDCl$_3$) δ 151.74 (C-4), 140.74 (C-6), 139.77 (C-1′), 137.98 (C-2), 137.53 (C-7a), 128.63 (C-3′, C-5′), 127.93 (C-2′, C-6′), 127.21 (C-4′, C-3a), 97.06 (C-7), 48.40 (*C*H(CH$_3$)$_2$), 45.20 (CH$_2$), 22.80 (2×CH$_3$). HR-MS (ESI) *m*/*z*: Calcd for $C_{16}H_{19}N_4$: [M1 +H]$^+$ = 267.1604, found 267.1610. Anal. Calcd for $C_{16}H_{18}N_4$: C, 72.15; H, 6.81; N, 21.04. Found: C, 72.29; H, 6.89; N, 20.79.

4.1.8.9. *N*-Benzyl-1-cyclopentyl-1*H*-imidazo[4,5-*c*]pyridin-4-amine (16i). This compound was synthesized according to the general procedure described above, upon reaction of **15d** with cyclopentyl bromide. Purification was effected using a mixture of dichloromethane/methanol (100/2, v/v) as the eluent to provide pure **16i** as a pale yellow oil, in 52% yield. ^{1}H NMR (600 MHz, $CDCl_3$) δ 7.84 (d, 1H, J = 5.9 Hz, H-6), 7.66 (s, 1H, H-2), 7.34 (d, 2H, J = 7.5 Hz, H-2′, H-6′), 7.24 (t, 2H, J = 7.5 Hz, H-3′, H-5′), 7.17 (t, 1H, J = 7.5 Hz, H-4′), 6.64 (d, 1H, J = 5.9 Hz, H-7), 5.77 (br s, 1H, D_2O exch, NH), 4.77 (d, 2H, J = 5.7 Hz, CH_2), 4.57 (m, 1H, H-1″), 2.22–2.15 (m, 2H, cyclopentyl-H), 1.96–1.89 (m, 2H, cyclopentyl-H), 1.87–1.81 (m, 2H, cyclopentyl-H), 1.76–1.70 (m, 2H, cyclopentyl-H). ^{13}C NMR (151 MHz, $CDCl_3$) δ 151.71 (C-4), 140.67 (C-6), 139.78 (C-1′), 138.64 (C-2), 137.99 (C-7a), 127.92 (C-2′, C-6′), 127.20 (C-4′), 97.30 (C-7), 57.54 (C-1″), 45.20 (CH_2), 32.55 (C-2″, C-5″), 24.05 (C-3″, C-4″). HR-MS (ESI) m/z: Calcd for $C_{18}H_{21}N_4$: $[M+H]^+$ = 293.1761, found 293.1766. Anal. Calcd for $C_{18}H_{20}N_4$: C, 73.94; H, 6.89; N, 19.17. Found: C, 74.14; H, 6.98; N, 18.83.

4.1.8.10. 4-(3,5-Dimethoxyphenoxy)-1-isopropyl-1*H*-imidazo[4,5-*c*]pyridine (16j) and 4-(3,5-dimethoxyphenoxy)-3-isopropyl-3*H*-imidazo[4,5-*c*]pyridine (17a). These compounds were synthesized according to the general procedure described above, upon reaction of **15e** with isopropyl bromide. Purification was effected using a mixture of dichloromethane/methanol (100/1, v/v) as the eluent to provide the pure isomers **16j** and **17a**.

Data for **16j***:* Yield 29%. White solid, mp 127–8 °C (Et_2O). ^{1}H NMR (600 MHz, $CDCl_3$) δ 8.00 (s, 1H, H-2), 7.95 (d, 1H, J = 5.7 Hz, H-6), 7.09 (d, 1H, J = 5.7 Hz, H-7), 6.44 (d, 2H, J = 2.2 Hz, H-2″, H-6″), 6.31 (t, 1H, J = 2.2 Hz, H-4′), 4.62 (septet, 1H, J = 6.7 Hz, C*H*$(CH_3)_2$), 3.75 (s, 6H, 2×OCH_3), 1.63 (d, 6H, J = 6.7 Hz, 2×CH_3). ^{13}C NMR (151 MHz, $CDCl_3$) δ 161.26 (C-3″, C-5″), 155.75 (C-1″), 155.61 (C-4), 140.72 (C-7a), 140.60 (C-2), 139.54 (C-6), 129.68 (C-3a), 102.49 (C-7), 100.30 (C-2″, C-6″), 97.41 (C-4″), 55.50 (2×OCH_3), 48.75 (*C*H$(CH_3)_2$), 22.76 (2×CH_3). HR-MS (ESI) m/z: Calcd for $C_{17}H_{20}N_3O_3$: $[M1+H]^+$ = 314.1499, found 314.1503. Anal. Calcd for $C_{17}H_{19}N_3O_3$: C, 65.16; H, 6.11; N, 13.41. Found: C, 64.98; H, 6.02; N, 13.69.

Data for **17a***:* Yield 36%. White solid, mp 135–6 °C (Et_2O). ^{1}H NMR (600 MHz, $CDCl_3$) δ 8.10 (s, 1H, H-2), 7.92 (d, 1H, J = 5.7 Hz, H-6), 7.41 (d, 1H, J = 5.7 Hz, H-7), 6.36 (d,2H, J = 2.2 Hz, H-2″, H-6″), 6.33 (t, 1H, J = 2.2 Hz, H-4″), 5.15 (septet, 1H, J = 6.7 Hz, C*H*$(CH_3)_2$), 3.76 (s, 6H, 2×OCH_3), 1.64 (d, 6H, J = 6.7 Hz, 2×CH_3). ^{13}C NMR (151 MHz, $CDCl_3$) δ 161.55 (C-3″, C-5″), 155.38 (C-1″), 152.26 (C-4), 150.11 (C-7a), 142.53 (C-2), 138.71 (C-6), 119.97 (C-3a), 111.65 (C-7), 99.85 (C-2″, C-6″), 97.36 (C-4″), 55.55 (2×OCH_3), 49.96 (*C*H$(CH_3)_2$), 23.71 (2×CH_3). HR-MS (ESI) m/z: Calcd for $C_{17}H_{20}N_3O_3$: $[M1+H]^+$ = 314.1499, found 314.1507. Anal. Calcd for $C_{17}H_{19}N_3O_3$: C, 65.16; H, 6.11; N, 13.41. Found: C, 65.34; H, 6.17; N, 13.24.

4.1.8.11. 1-Cyclopentyl-4-(3,5-dimethoxyphenoxy)-1*H*-imidazo[4,5-*c*]pyridine (16k) and 3-cyclopentyl-4-(3,5-dimethoxyphenoxy)-3*H*-imidazo[4,5-*c*]pyridine (17b). These compounds were synthesized according to the general procedure described above, upon reaction of **15e** with cyclopentyl bromide. Purification was effected using a mixture of dichloromethane/methanol (100/1, v/v) as the eluent to provide the pure isomers **16k** and **17b**.

Data for **16k***:* Yield 44%. White solid, mp 165–6 °C (Et_2O). ^{1}H NMR (600 MHz, $CDCl_3$) δ 7.96 (s, 1H, H-2), 7.94 (d, 1H, J = 5.7 Hz, H-6), 7.09 (d, 1H, J = 5.7 Hz, H-7), 6.43 (d, 2H, J = 2.2 Hz, H-2″, H-6″), 6.31 (t, 1H, J = 2.2 Hz, H-4″), 4.72 (m, 1H, H-1′), 3.76 (s, 6H, 2×OCH_3), 2.33–2.26 (m, 2H, cyclopentyl-H), 2.06–1.99 (m, 2H, cyclopentyl-H), 1.96–1.90 (m, 2H, cyclopentyl-H), 1.85–1.81 (m, 2H, cyclopentyl-H). ^{13}C NMR (151 MHz, $CDCl_3$) δ 161.24 (C-3″, C-5″), 156.77 (C-7a), 155.77 (C-1″), 155.54 (C-4), 141.18 (C-2), 139.47 (C-6), 129.73 (C-3a), 102.72 (C-7), 100.26 (C-2″, C-6″), 97.37 (C-4″), 57.77 (C-1′), 55.47(2×OCH_3), 32.55 (C-2′, C-5′), 24.00 (C-3′, C-4′). HR-MS (ESI) m/z: Calcd for $C_{19}H_{22}N_3O_3$: $[M1+H]^+$ = 340.1656, found 340.1662. Anal. Calcd for $C_{19}H_{21}N_3O_3$: C, 67.24; H, 6.24; N, 12.38. Found: C, 67.01; H, 6.14; N, 12.55.

Data for **17b***:* Yield 44%. White solid, mp 139–140 °C (Et_2O). ^{1}H NMR (600 MHz, $CDCl_3$) δ 8.06 (s, 1H, H-2), 7.91 (d, 1H, J = 5.7 Hz, H-6), 7.40 (d, 1H, J = 5.7 Hz, H-7), 6.36 (d, 2H, J = 2.2 Hz, H-2″, H-6″), 6.33 (t, 1H, J = 2.2 Hz, H-4″), 5.23 (m, 1H, H-1′), 3.76 (s, 6H, 2×OCH_3), 2.33–2.26 (m, 2H, cyclopentyl-H), 2.06–1.99 (m, 2H, cyclopentyl-H), 1.91–1.84 (m, 2H, cyclopentyl-H), 1.80–1.74 (m, 2H, cyclopentyl-H). ^{13}C NMR (151 MHz, $CDCl_3$) δ 161.51 (C-3″, C-5″), 155.47 (C-1″), 152.42 (C-4), 150.24 (C-7a), 143.01 (C-2), 138.67 (C-6), 120.43 (C-3a), 111.62 (C-7), 99.79 (C-2″, C-6″), 97.25 (C-4″), 59.23 (C-1′), 55.51 (2×OCH_3), 33.64 (C-2′, C-5′), 23.86 (C-3′, C-4′). HR-MS (ESI) m/z: Calcd for $C_{19}H_{22}N_3O_3$: $[M1+H]^+$ = 340.1656, found 340.1664. Anal. Calcd for $C_{19}H_{21}N_3O_3$: C, 67.24; H, 6.24; N, 12.38. Found: C, 66.98; H, 6.09; N, 12.66.

4.1.9. General procedure for the synthesis of compounds 18b–c

Ammonium formate (150 mg, 2.5 mmol) and 10% Pd/C (70 mg) were added into a solution of the benzylamines **16h** or **16i** (0.25 mmol) in methanol (5 mL), under argon, and this reaction mixture was refluxed for 48 h. An additional amount (300 mg, 5.0 mmol) of ammonium formate was added and the reflux was continued for 48 h. Upon completion of the reaction, the solution was filtered through a celite pad to remove the catalyst and the filtrate was evaporated to dryness. The crude product was purified by column chromatography (silica gel) to provide pure aminoderivatives **18b** and **18c**.

4.1.9.1. 1-Isopropyl-1*H*-imidazo[4,5-*c*]pyridin-4-amine (18b). This compound was synthesized according to the general procedure described above, starting from **16h**. Purification was effected using a mixture of dichloromethane/methanol (9/1, v/v) as the eluent to provide pure **18b** as a pale yellow oil, in 43% yield. ^{1}H NMR (600 MHz, $(CD_3)_2CO$) δ 8.12 (s, 1H, H-2), 7.71 (d, 1H, J = 6.0 Hz, H-6), 6.92 (d,1H, J = 6.0 Hz, H-7), 6.29 (br s, 2H, D_2O exch, NH_2), 4.73 (septet, 1H, J = 6.7 Hz, C*H*$(CH_3)_2$), 1.60 (d, 6H, J = 6.7 Hz, 2×CH_3). ^{13}C NMR (151 MHz, $(CD_3)_2CO$) δ 153.01 (C-4), 140.53 (C-2), 139.13 (C-7a), 138.87 (C-6), 128.39 (C-3a), 98.48 (C-7), 49.18 (*C*H$(CH_3)_2$), 22.76 (2×CH_3). HR-MS (ESI) m/z: Calcd for $C_9H_{13}N_4$: $[M1+H]^+$ = 177.1135, found 177.1130. Anal. Calcd for $C_9H_{12}N_4$: C, 61.34; H, 6.86; N, 31.79. Found: C, 61.52; H, 6.93; N, 31.49.

4.1.9.2. 1-Cyclopentyl-1*H*-imidazo[4,5-*c*]pyridin-4-amine (18c). This compound was synthesized according to the general procedure described above, starting from **16i**. Purification was effected using a mixture of dichloromethane/methanol (100/8, v/v) as the eluent to provide pure **18c** as a pale yellow oil, in 82% yield. ^{1}H NMR (600 MHz, $(CD_3)_2CO$) δ 8.12 (s, 1H, H-2), 7.72 (d, 1H, J = 6.0 Hz, H-6), 6.95 (d,1H, J = 6.0 Hz, H-7), 6.44 (br s, 2H, D_2O exch, NH_2), 4.87 (m, 1H, H-1′), 2.34–2.26 (m, 2H, cyclopentyl-H), 2.08–2.00 (m, 2H, cyclopentyl-H), 1.97–1.91 (m, 2H, cyclopentyl-H), 1.84–1.77 (m, 2H, cyclopentyl-H). ^{13}C NMR (151 MHz, $(CD_3)_2CO$) δ 152.81 (C-4), 141.24 (C-2), 139.75 (C-7a), 138.14 (C-6), 128.44 (C-3a), 98.76 (C-7), 58.28 (C-1′), 33.04 (C-2′, C-5′), 24.64 (C-3′, C-4′). HR-MS (ESI) m/z: Calcd for $C_{11}H_{15}N_4$: $[M1+H]^+$ = 203.1291, found 203.1284. Anal. Calcd for $C_{11}H_{14}N_4$: C, 65.32; H, 6.98; N, 27.70. Found: C, 65.44; H, 7.04; N, 27.51.

4.2. Combinatorial design-molecular docking calculations

4.2.1. Ligand enumeration—preparation

Based on the scaffold of 3-deazaadenine, we enumerated a virtual combinatorial library using our in-house fragment library

containing 200 chemical fragments. Moreover, we defined 2 positions for substitutions (1 and 4) combining 0 to 2 methylene groups as linkers between the fragment and the core. Thus the intensity of the new virtual chemical library enumerated 1200 compounds. All ligands were prepared using the ligprep module as implemented on Schrodinger Suite 2014. The geometries of the generated structures are optimized using a restricted version of the MacroModel™ computational program, bmin, or a short conformational search is performed to relax the structure into 3 dimensions while strongly encouraging chiral centers to adopt the proper chirality (if the structure is highly strained). For the mono 4-substitued analogues of 3-deaza adenine, both 1NH and 3NH tautomers were generated for further docking calculations.

4.2.2. Virtual screening

The modeled structure of FcyB transporter is already described by our group,[15] and prepared for Virtual Screening using the protein preparation workflow as implemented on Schrodinger suite 2014. Glide energy grids were generated using the Receptor Grid Generation panel on Maestro software with default values. Glide software was utilized for virtual screening using the SP protocol. The enumerated database created passed through virtual screening and only the first 2% (40 structures) of ligands based on GlideScore stored for Induced Fit Docking.

4.2.3. Induced Fit Docking

All selected molecules for synthesis were passed through exhaustive molecular docking calculations using the IFD protocol (Induced Fit Docking protocol 2015–2, Glide version 6.4, Prime version 3.7, Schrödinger, LLC, 2015),[27,28] which is intended to circumvent the inflexible binding site and accounts for the side-chain or backbone movements, or both, upon ligand binding. In the first stage of the IFD protocol, softened-potential docking step, 20 poses per ligand were retained. In the second step, for each docking pose, a full cycle of protein refinement was performed, with Prime 3.7 (Prime, version 3.7, Schrödinger, LLC) on all residues having at least one atom within 8 Å of an atom in any of the 20 ligand poses. The Prime refinement starts with a conformational search and minimization of the side-chains of the selected residues and after convergence to a low-energy solution, an additional minimization of all selected residues (side-chain and backbone) is performed with the truncated-Newton algorithm using the OPLS parameter set and a surface Generalized Born implicit solvent model. The obtained complexes are ranked according to Prime calculated energy (molecular mechanics and solvation), and those within 30 kcal/mol of the minimum energy structure are used in the last step of the process, redocking with Glide 6.4 (Glide, version 6.4, Schrödinger, LLC, 2015) using standard precision and scoring. In the final round, the ligands used in the first docking step are redocked into each of the transporter structures retained from the refinement step. The final ranking of the complexes is done by a composite score which accounts for the transporter–ligand interaction energy (GlideScore) and solvation energies (Prime energy).

4.3. *Aspergillus* manipulations

Standard complete and minimal media (MM) for *A. nidulans* were used. Media and supplemented auxotrophies were at the concentrations given in http://www.fgsc.net. 10 mM $NaNO_3$ was used as a nitrogen source. Inhibitors are added in MM dissolved in DMSO at 500 μM. Transformations were performed as described previously.[29] Transformants of the Δ7 master mutant, arising from single-copy plasmid integration events of vectors carrying the either *fcyB* or the *azgA* gene, in addition to a wild-type *pabA1* selection marker, were obtained by complementation of the *pabA1* auxotrophy. The Δ7 master mutant contains total genetic deletion of all major nucleobase/nucleoside transporters (*ΔfcyB::argB ΔazgA, ΔuapA, ΔuapC::AfpyrG, ΔfurD::riboB ΔfurA::riboB, ΔcntA::riboB, pantoB100, pabA1*), in addition to *pabA1* auxotrophy. Confirmation of single copy integrations, introducing intact *fcyB* or *azgA* genes, was obtained by Southern and PCR analyses. *azgA*- and *fcyB*-containing vectors,[16,17] and the Δ7 mutant strain[13] have been described before. In the case of *fcyB*, transcription is driven by the *uapA* promoter for obtaining sufficient protein levels for functional assays.[17] AzgA transcription is driven by its nature promoter.

4.4. Transport assays

Transport assays for measuring the activity of purine transporters, such as FcyB, AzgA or UapA, is carried out in germinating conidiospores, as recently described in detail.[13] For transport competition assays, 0.5 μM of ^{3}H-radiolabelled substrate (adenine, hypoxanthine or xanthine) is added in a mix with 1000-fold excess 3-deazaadenine analogues (500 μM).[13] Assays are terminated after 1 min by freezing, immediate centrifugation and washing of cells. K_i values are estimated from IC_{50} measurements using the Cheng and Prussof equation [$K_i = IC_{50}/1 + [S]/K_m$, where [S] is the fixed concentration of radiolabeled substrate used] and analyzed by the GraphPad Prism software. All experiments are carried out at three times, with each assays performed in triplicate. Standard deviation in all cases is less than 30%. Radiolabeled purines used are: [2,8-^{3}H]-adenine 20.0 Ci/mmol, [2,8-^{3}H]-hypoxanthine 27.7 Ci/mmol or [8-^{3}H]-xanthine 22.8 Ci/mmol, all from Moravek Biochemicals.

Acknowledgements

This research was co-supported by the European Union (European Social Fund) and Greek national funds through the Operational Program 'Education and Lifelong Learning' of the National Strategic Reference Framework-Research Funding Program: THALES, investing in knowledge society through the European Social Fund.

References and notes

1. Kwon-Chung, K. J.; Sugui, J. A. *PLoS Pathog.* **2013**, *9*, e1003743.
2. Moye-Rowley, W. S. *Front. Microbiol.* **2015**, *6*, 70.
3. Odds, F. C.; Brown, A. J.; Gow, N. A. *Trends Microbiol.* **2003**, *11*, 272.
4. Wiederhold, N. P.; Patterson, T. F. *Curr. Opin. Infect. Dis.* **2015**, *28*, 539.
5. Lamping, E.; Baret, P. V.; Holmes, A. R.; Monk, B. C.; Goffeau, A.; Cannon, R. D. *Fungal Genet. Biol.* **2010**, *47*, 127.
6. Cannon, R. D.; Lamping, E.; Holmes, A. R.; Niimi, K.; Baret, P. V.; Keniya, M. V.; Tanabe, K.; Niimi, M.; Goffeau, A.; Monk, B. C. *Clin. Microbiol. Rev.* **2009**, *22*, 291.
7. Prasad, R.; Rawal, M. K. *Front. Pharmacol.* **2014**, *5*, 202.
8. Paluszynski, J. P.; Klassen, R.; Rohe, M.; Meinhardt, F. *Yeast* **2006**, *23*, 707.
9. Krypotou, E.; Evangelidis, T.; Bobonis, J.; Pittis, A. A.; Gabaldon, T.; Scazzocchio, C.; Mikros, E.; Diallinas, G. *Mol. Microbiol.* **2015**, *96*, 927.
10. Pantazopoulou, A.; Diallinas, G. *FEMS Microbiol. Rev.* **2007**, *31*, 657.
11. Diallinas, G.; Gournas, C. *Channels* **2008**, *2*, 363.
12. Diallinas, G. *Front. Pharmacol.* **2014**, *5*, 207.
13. Krypotou, E.; Diallinas, G. *Fungal Genet. Biol.: FG & B* **2014**, *63*, 1.
14. Kosti, V.; Lambrinidis, G.; Myrianthopoulos, V.; Diallinas, G.; Mikros, E. *PLoS ONE* **2012**, *7*, e41939.
15. Krypotou, E.; Kosti, V.; Amillis, S.; Myrianthopoulos, V.; Mikros, E.; Diallinas, G. *J. Biol. Chem.* **2012**, *287*, 36792.
16. Krypotou, E.; Lambrinidis, G.; Evangelidis, T.; Mikros, E.; Diallinas, G. *Mol. Microbiol.* **2014**, *93*, 129.
17. Vlanti, A.; Diallinas, G. *Mol. Microbiol.* **2008**, *68*, 959.
18. Connon, S. J.; Hegarty, A. F. *Eur. J. Org. Chem.* **2004**, *2004*, 3477.
19. Searls, T.; McLaughlin, L. W. *Tetrahedron* **1999**, *55*, 11985.
20. Yin, X.; Schneller, S. W. *Nucleosides Nucleotides Nucleic Acids* **2004**, *23*, 67.
21. Dvořáková, H.; Holý, A.; Votruba, I.; Masojídková, M. *Collect. Czech. Chem. Commun.* **1993**, *58*, 629.

22. Huang, L. K.; Cherng, Y. C.; Cheng, Y. R.; Jang, J. P.; Chao, Y. L.; Cherng, Y. J. *Tetrahedron* **2007**, *63*, 5323.
23. Sander, K.; Kottke, T.; Tanrikulu, Y.; Proschak, E.; Weizel, L.; Schneider, E. H.; Seifert, R.; Schneider, G.; Stark, H. *Bioorg. Med. Chem.* **2009**, *17*, 7186.
24. Crey-Desbiolles, C.; Kotera, M. *Bioorg. Med. Chem.* **2006**, *14*, 1935.
25. Schwoch, S.; Kramer, W.; Neidlein, R.; Suschitzky, H. *Helv. Chim. Acta* **1994**, *77*, 2175.
26. Krenitsky, T. A.; Rideout, J. L.; Chao, E. Y.; Koszalka, G. W.; Gurney, F.; Crouch, R. C.; Cohn, N. K.; Wolberg, G.; Vinegar, R. *J. Med. Chem.* **1986**, *29*, 138.
27. Sherman, W.; Day, T.; Jacobson, M. P.; Friesner, R. A.; Farid, R. *J. Med. Chem.* **2006**, *49*, 534.
28. Sherman, W.; Beard, H. S.; Farid, R. *Chem. Biol. Drug Des.* **2006**, *67*, 83.
29. Koukaki, M.; Giannoutsou, E.; Karagouni, A.; Diallinas, G. *J. Microbiol. Methods* **2003**, *55*, 687.

Παράρτημα

I. Τεχνικές στις οποίες εξασκήθηκα:

Ασκήθηκα στις εξής τεχνικές κατά τη διάρκεια της εκπόνησης της διετούς μου διπλωματικής εργασίας:

- ηλεκτροφόρηση
- αλυσιδωτή αντίδραση
- κλωνοποίηση
- κινητικός χαρακτηρισμός μέσω πρόσληψης ραδιενεργού υποστρώματος
- δοκιμασίες ανάπτυξης
- εξαγωγή μορίων DNA
- εξαγωγή μορίων RNA
- southern
- northern
- μικροσκοπία φθορισμού
- γονιδιακές απαλοιφές μέσω γραμμικών κασετών
- κατευθυνόμενη μεταλλαξογένεση

II. Στελέχη τα οποία κατασκεύασα:

	Γονότυπος
1	uapAΔ uapCΔ::AFpyrG azgAΔ fcyBΔ::argB furDΔ::AFriboB furAΔ::AFriboB cntAΔ::AFriboB pantoB100 pabaA1 pGEM-gpdAp-FcyD-trpC-pantoB (8)
2	uapAΔ uapCΔ::AFpyrG azgAΔ fcyBΔ::argB furDΔ::AFriboB furAΔ::AFriboB cntAΔ::AFriboB pantoB100 pabaA1 pGEM-gpdAp-FcyD-trpC-pantoB (10)
3	uapAΔ uapCΔ::AFpyrG azgAΔ fcyBΔ::argB furDΔ::AFriboB furAΔ::AFriboB cntAΔ::AFriboB pantoB100 pabaA1 pGEM-gpdAp-FcyD-F167W-trpC-pantoB (2)
4	uapAΔ uapCΔ::AFpyrG azgAΔ fcyBΔ::argB furDΔ::AFriboB furAΔ::AFriboB cntAΔ::AFriboB pantoB100 pabaA1 pGEM-gpdAp-FcyD-F167W-trpC-pantoB (4)
5	uapAΔ uapCΔ::AFpyrG azgAΔ fcyBΔ::argB furDΔ::AFriboB furAΔ::AFriboB cntAΔ::AFriboB pantoB100 pabaA1 pGEM-gpdAp-FcyD-S171N-trpC-pantoB (2)
6	uapAΔ uapCΔ::AFpyrG azgAΔ fcyBΔ::argB furDΔ::AFriboB furAΔ::AFriboB cntAΔ::AFriboB pantoB100 pabaA1 pGEM-gpdAp-FcyD-S171N-trpC-pantoB (6)
7	uapAΔ uapCΔ::AFpyrG azgAΔ fcyBΔ::argB furDΔ::AFriboB furAΔ::AFriboB cntAΔ::AFriboB pantoB100 pabaA1 pGEM-gpdAp-FcyD-L356N-trpC-pantoB (4)
8	uapAΔ uapCΔ::AFpyrG azgAΔ fcyBΔ::argB furDΔ::AFriboB furAΔ::AFriboB cntAΔ::AFriboB pantoB100 pabaA1 pGEM-gpdAp-FcyD-L356N-trpC-pantoB (6)
9	uapAΔ uapCΔ::AFpyrG azgAΔ fcyBΔ::argB furDΔ::AFriboB furAΔ::AFriboB cntAΔ::AFriboB pantoB100 pabaA1 pGEM-gpdAp-FcyD-A358P-trpC-pantoB (4)
10	uapAΔ uapCΔ::AFpyrG azgAΔ fcyBΔ::argB furDΔ::AFriboB furAΔ::AFriboB cntAΔ::AFriboB pantoB100 pabaA1 pGEM-gpdAp-FcyD-A358P-trpC-pantoB (3)
11	uapAΔ uapCΔ::AFpyrG azgAΔ fcyBΔ::argB furDΔ::AFriboB furAΔ::AFriboB cntAΔ::AFriboB pantoB100 pabaA1 pGEM-gpdAp-FcyD-S359N-trpC-pantoB (3)
12	uapAΔ uapCΔ::AFpyrG azgAΔ fcyBΔ::argB furDΔ::AFriboB furAΔ::AFriboB cntAΔ::AFriboB pantoB100 pabaA1 pGEM-gpdAp-FcyD-S359N-trpC-pantoB (5)
13	uapAΔ uapCΔ::AFpyrG azgAΔ fcyBΔ::argB furDΔ::AFriboB furAΔ::AFriboB cntAΔ::AFriboB pantoB100 pabaA1 pGEM-gpdAp-FcyD-L356N/A358P-trpC-pantoB (2)

14	uapAΔ uapCΔ::AFpyrG azgAΔ fcyBΔ::argB furDΔ::AFriboB furAΔ::AFriboB cntAΔ::AFriboB pantoB100 pabaA1 pGEM-gpdAp-FcyD-L356N/S359N-trpC-pantoB (2)
15	uapAΔ uapCΔ::AFpyrG azgAΔ fcyBΔ::argB furDΔ::AFriboB furAΔ::AFriboB cntAΔ::AFriboB pantoB100 pabaA1 pGEM-gpdAp-FcyD-L356N/S359N-trpC-pantoB (6)
16	uapAΔ uapCΔ::AFpyrG azgAΔ fcyBΔ::argB furDΔ::AFriboB furAΔ::AFriboB cntAΔ::AFriboB pantoB100 pabaA1 pGEM-gpdAp-FcyD-A358P/S359N-trpC-pantoB (2)
17	uapAΔ uapCΔ::AFpyrG azgAΔ fcyBΔ::argB furDΔ::AFriboB furAΔ::AFriboB cntAΔ::AFriboB pantoB100 pabaA1 pGEM-gpdAp-FcyD-A358P/S359N-trpC-pantoB (3)
18	uapAΔ uapCΔ::AFpyrG azgAΔ fcyBΔ::argB furDΔ::AFriboB furAΔ::AFriboB cntAΔ::AFriboB pantoB100 pabaA1 pGEM-gpdAp-FcyA-trpC-pantoB (2)
19	uapAΔ uapCΔ::AFpyrG azgAΔ fcyBΔ::argB furDΔ::AFriboB furAΔ::AFriboB cntAΔ::AFriboB pantoB100 pabaA1 pGEM-gpdAp-FcyA-trpC-pantoB (8)
20	uapAΔ uapCΔ::AFpyrG azgAΔ fcyBΔ::argB furDΔ::AFriboB furAΔ::AFriboB cntAΔ::AFriboB pantoB100 pabaA1 pbs-gpdAmini-FcyB-argB (1)
21	uapAΔ uapCΔ::AFpyrG azgAΔ fcyBΔ::argB furDΔ::AFriboB furAΔ::AFriboB cntAΔ::AFriboB pantoB100 pabaA1 pGEM-gpdAp-FcyC-trpC-pantoB (4)
22	uapAΔ uapCΔ::AFpyrG azgAΔ fcyBΔ::argB furDΔ::AFriboB furAΔ::AFriboB cntAΔ::AFriboB pantoB100 pabaA1 pGEM-gpdAp-FcyE-trpC-pantoB (1)
23	uapAΔ uapCΔ::AFpyrG azgAΔ fcyBΔ::argB furDΔ::AFriboB furAΔ::AFriboB cntAΔ::AFriboB pantoB100 pabaA1 pGEM-gpdAp-FcyE-trpC-pantoB (3)
24	uapAΔ uapCΔ::AFpyrG azgAΔ fcyBΔ::argB furDΔ::AFriboB furAΔ::AFriboB cntAΔ::AFriboB pantoB100 pabaA1 pGEM-gpdAp-FcyD-L356N/A358P/S359N-trpC-pantoB (2)
25	uapAΔ uapCΔ::AFpyrG azgAΔ fcyBΔ::argB furDΔ::AFriboB furAΔ::AFriboB cntAΔ::AFriboB pantoB100 pabaA1 pGEM-gpdAp-FcyD-L356N/A358P/S359N-trpC-pantoB (4)
26	pttAΔ::pabaA AN1186::AFpyrG ΔnkuA::argB pyroA4 riboB2 (24)
27	pttAΔ::pabaA AN1186::AFpyrG ΔnkuA::argB pyroA4 riboB2 (39)
28	AN6783Δ::AFpyrG nkuAΔ::argB riboB2 pyroA4 pyrG89

Ευχαριστίες

Θα ήθελα να ευχαριστήσω θερμά τον καθηγητή Γ. Διαλλινά για την ευκαιρία που μου έδωσε να εκπονήσω τη διπλωματική μου εργασία στο εργαστήριο του και να συμμετάσχω σε αξιόλογες εργασίες, οι οποίες κατέληξαν σε δημοσιεύσεις και μου προσέφεραν πολλές και σημαντικές γνώσεις. Ο κ. Διαλλινάς συνέβαλλε ενεργά στη πολύπλευρη βελτίωση μου και αυτό είναι κάτι για το οποίο είμαι πραγματικά ευγνώμων.

Ευχαριστώ επίσης τον επιστημονικό συνεργάτη Σ. Αμίλλη για την ανεκτίμητη βοήθεια που μου παρείχε απλόχερα και για την πολύ σημαντική συμβολή του στην εργασία μου με τίτλο: Cryptic purine transporters in *Aspergillus nidulans* reveal the role of specific residues in the evolution of specificity in the NCS1 family.

Ευχαριστώ τα πρώην και νην μέλη του εργαστηρίου: τους φοιτητές Μπομπόνη Ιάκωβο, Καρβελά Ηλιάνα, Χοροζίαν Κοάρ, Μπαλάσκα Σοφία, Παπαδάκη Γεωργία και Μπαρτζώκα Γιάννη τους διδακτορικούς Ευαγγελινό Μίνωα, Κρυπωτού Αιμιλία και Μαρτζούκου Όλγα και τον μεταπτυχιακό φοιτητή Καπετανάκη Γιώργο για την υποστήριξη, την βοήθεια τους καθώς και για την αρμονική συμβίωση μας στο εργαστήριο. Υπήρξε ένα πολύ ευχάριστο κλίμα μεταξύ όλων μας και το οποίο ήταν πολύ σημαντικό για να διεξάγεται πιο αρμονικά και πιο εύκολα η καθημερινή μας δουλεία.